
Theoretical Benefit and Limitation of Diffusion Language Model

Guhao Feng^{*1} Yihan Geng^{*1} Jian Guan² Wei Wu² Liwei Wang¹ Di He¹

Abstract

Diffusion language models have emerged as a promising approach for text generation. One would naturally expect this method to be an efficient replacement for autoregressive models since multiple tokens can be sampled in parallel during each diffusion step. However, its efficiency-accuracy trade-off is not yet well understood. In this paper, we present a rigorous theoretical analysis of a widely used type of diffusion language model, the Masked Diffusion Model (MDM), and find that its effectiveness heavily depends on the target evaluation metric. Under mild conditions, we prove that when using perplexity as the metric, MDMs can achieve near-optimal perplexity in sampling steps regardless of sequence length, demonstrating that efficiency can be achieved without sacrificing performance. However, when using the sequence error rate—which is important for understanding the “correctness” of a sequence, such as a reasoning chain—we show that the required sampling steps must scale linearly with sequence length to obtain “correct” sequences, thereby eliminating MDM’s efficiency advantage over autoregressive models. Our analysis establishes the first theoretical foundation for understanding the benefits and limitations of MDMs. All theoretical findings are supported by empirical studies.

1. Introduction

Diffusion models (Ho et al., 2020; Song et al., 2021b) have emerged as a powerful paradigm in generative modeling, establishing state-of-the-art performance in image synthesis (Karras et al., 2022; Song et al., 2021a). Their extension to discrete domains has opened new possibilities for generating sequences, such as natural language (Campbell et al., 2022; Dieleman et al., 2022; Zheng et al., 2023; Lou et al., 2024; Campbell et al., 2024; Lovelace et al., 2024) and biological sequences (Rastogi et al., 2022; Vignac et al., 2022;

Sun & Yang, 2023; Avdeyev et al., 2023). Among various discrete diffusion architectures, masked diffusion models (MDMs) (Shi et al., 2024; Sahoo et al., 2024; Ou et al., 2024)—which generate sequences by iteratively converting masks to tokens—have emerged as a prominent approach and demonstrated competitive performance across diverse language modeling tasks.

While auto-regressive models generate sequences token-by-token, discrete diffusion models can generate multiple tokens simultaneously during each step (reverse process). Therefore, it is natural to hypothesize that this parallel sampling improves generation efficiency. However, we argue that reaching a conclusion requires considering both computational cost and generation quality. Specifically, we pose the following question: do discrete diffusion models achieve superior efficiency when the generated content meets an acceptable quality standard? There may be multiple answers to this question. If diffusion models require fewer neural network executions while maintaining quality, they can offer better acceleration. Conversely, if their execution count is comparable to or exceeds that of auto-regressive models, diffusion language models may not be a better choice.

To answer the above question, we leverage two complementary metrics to evaluate the efficiency of MDMs in language modeling. The first metric, *token error rate* (TER), quantifies token-level accuracy, which correlates with the fluency of the generated text. In practice, *perplexity* is a widely used metric for measuring token-level errors of language models (Jelinek et al., 1977; Devlin et al., 2019); thus, we define the metric of TER by perplexity in this paper. The second metric, *sequence error rate* (SER), evaluates the correctness of an entire sequence, which is crucial for reasoning tasks requiring logically correct sequences. We provide a natural definition of SER that reflects the correctness of the whole sequence. Together, these metrics enable a comprehensive evaluation of the efficiency of MDMs under both token-level and sequence-level metrics. We first provide a positive theoretical result regarding TER. We prove that under mild conditions, MDMs can achieve near-optimal TER with sampling steps regardless of the sequence length L . Compared to the auto-regressive model, which must be executed L times to generate the sequence, MDMs demonstrate substantial efficiency gains, especially when the generation length is long.

^{*}Equal contribution ¹Peking University ²Ant Group.

However, we show that this efficiency advantage diminishes when SER is considered. We theoretically prove that to achieve a low SER, the number of required sampling steps for MDMs scales at least linearly with sequence length. Intuitively, this limitation arises from the fact that SER, as a metric for the entire sequence, requires the generated sequence to be free of any error in the whole sequence, which forces MDMs to sample only a small number of tokens per step to mitigate such inconsistencies. As a result, the number of required sampling steps can be significant. It is notable that each MDM sampling step usually incurs a higher computational cost than an auto-regressive step under the same architecture, thus MDMs offer no efficiency advantage under this metric.

Finally, we validate our theoretical findings through comprehensive experiments. Our experiments examine MDMs trained on formal languages, including n -gram languages and Hidden Markov Models (HMMs), systematically analyzing the relationship between performance and efficiency under both TER and SER metrics. Additional experiments on natural language tasks, including TER evaluation on text generation and SER assessment on the GSM8k dataset (Cobbe et al., 2021), corroborate our theoretical predictions: while achieving low SER necessitates substantial sampling steps, relatively few steps suffice for TER. These results provide practical guidance for deploying diffusion language models across different applications.

2. Related Work

Discrete Diffusion Models. The auto-regressive paradigm has achieved significant success in language modeling (Dai, 2019; Floridi & Chiriatti, 2020; Achiam et al., 2023). However, its left-to-right, token-by-token generation approach is not without limitations. Notably, it faces challenges such as restricted controllability (Zhang et al., 2023) and inefficiencies in inference speed (Leviathan et al., 2023). To overcome these drawbacks, inspired by the success of diffusion models in image generation (Sohl-Dickstein et al., 2015; Song et al., 2021a; Karras et al., 2022) researchers have adapted these techniques for NLP tasks (Austin et al., 2021; He et al., 2022; Chen et al., 2022; Meng et al., 2022; Ye et al., 2023; Gulrajani & Hashimoto, 2023; Zhang et al., 2024). Discrete diffusion models, in particular, have shown promising results, achieving comparable performance with auto-regressive models across a range of NLP benchmarks.

Discrete diffusion models can be categorized based on the initialization strategy of the reverse process: (1) reverse processes that begin with masked sequences and (2) reverse processes that start with sequences of tokens sampled randomly from the vocabulary. The first category, termed *masked diffusion models* (MDMs), includes models such as SEDD Absorb (Lou et al., 2024) and its streamlined variants in

subsequent works (Sahoo et al., 2024; Zhao et al., 2024; Shi et al., 2024; Ou et al., 2024; Zheng et al., 2024). The second category encompasses models like SEDD Uniform (Lou et al., 2024), as well as extensions introduced in follow-up studies (Campbell et al., 2024). Notably, Gat et al. (2024); Davis et al. (2024) and Campbell et al. (2024) further extend flow-matching to the discrete domain, with differing initialization strategies: the former employs masked sequences, while the latter utilizes a customized distribution for the reverse process.

Masked Diffusion Models. Among the two primary classes of discrete diffusion models, MDMs have consistently demonstrated superior performance and scalability (Lou et al., 2024; Campbell et al., 2024). For instance, in Lou et al. (2024), the masked variant of SEDD significantly outperforms its uniform counterpart across a range of benchmarks. Similarly, Campbell et al. (2024) reports that the masked variant achieves better results in most language tasks. Furthermore, recent advancements have successfully scaled MDMs to over 1 billion parameters (Gat et al., 2024; Nie et al., 2024; Gong et al., 2024; Shi et al., 2024), underscoring their robustness and adaptability to large-scale NLP models. In this paper, we focus on MDMs, and our theoretical contributions can be applied to all MDMs, including the masked variant of discrete flow matching.

Various Metrics in NLP Tasks. Evaluation metrics in NLP tasks are inherently tied to the specific objectives and requirements of their respective domains. For general language modeling tasks, perplexity (Jelinek et al., 1977; Devlin et al., 2019) remains the metric of choice due to its ability to capture a model’s predictive performance effectively. However, domain-specific tasks often demand more specialized evaluation criteria. For instance, in machine translation (Bahdanau, 2014; Wu et al., 2016), the BLEU score is widely regarded as a standard measure of translation quality (Papineni et al., 2002), while text generation tasks (Sutskever, 2014) frequently rely on metrics such as ROUGE to assess output fidelity (Lin, 2004). Similarly, tasks requiring reasoning (Wei et al., 2022b), such as mathematics (Bubeck et al., 2023) or code generation (Roziere et al., 2023; Ouyang et al., 2023), commonly adopt accuracy as an intuitive and straightforward measure of success.

3. Masked Diffusion Language Model

Without loss of generality, we study the sequence generation task where the sequence length is upper bounded by L . Let \mathcal{V} denote the vocabulary. The MDM (Lou et al., 2024; Shi et al., 2024; Gong et al., 2024; Sahoo et al., 2024) extends the vocabulary \mathcal{V} by introducing a special mask token $[m]$. The forward diffusion process progressively transforms an initial sequence $x_0 = (x_0^1, x_0^2, \dots, x_0^L) \in \mathcal{V}^L$ into a fully masked sequence $x_1 = ([m], [m], \dots, [m])$

by independently masking each token according to a pre-defined schedule. Conversely, the reverse process defines a generative model that reconstructs a sequence by iteratively modifying a fully/partially masked sequence. Below, we formally define both the forward and reverse processes.

3.1. Forward Process

Given a sequence \mathbf{x}_0 and a masking schedule α_t , the distribution of the sequence \mathbf{x}_t at time $t \in [0, 1]$ is expressed as:

$$q_{t|0}(\mathbf{x}_t|\mathbf{x}_0) = \prod_{i=0}^{L-1} q_{t|0}(x_t^i|x_0^i), \quad (1)$$

where $q_{t|0}(x_t^i|x_0^i) = \begin{cases} \alpha_t, & x_t^i = x_0^i, \\ 1 - \alpha_t, & x_t^i = [m]. \end{cases}$

The masking schedule α_t is designed such that $\alpha_0 = 1$, ensuring that the sequence remains unmasked at the start of the process. Similar to the continuous diffusion methods (Ho et al., 2020; Song et al., 2021a; Karras et al., 2022), we set $\alpha_1 = 0$ (or a value approaching zero), ensuring the sequence is fully masked at the end of the forward process.

3.2. Reverse Process

The reverse process reconstructs a sequence from a masked version by reversing the forward dynamics. Given the sequence at time t and the original sequence \mathbf{x}_0 , the conditional distribution of the sequence at time $s < t$, is defined as:

$$q_{s|t,0}(x_s^i|\mathbf{x}_t, \mathbf{x}_0) = \frac{1 - \alpha_s}{1 - \alpha_t} \delta_{x_t^i}(x_s^i) + \frac{\alpha_s - \alpha_t}{1 - \alpha_t} \delta_{x_0^i}(x_s^i),$$

where $\delta_x(y)$ is the Kronecker delta function. Marginalizing over \mathbf{x}_0 yields the true reverse process $q(\mathbf{x}_s|\mathbf{x}_t)$:

$$q_{s|t}(\mathbf{x}_s|\mathbf{x}_t) = \prod_{i=0}^{L-1} q_{s|t}(x_s^i|\mathbf{x}_t), \quad \text{where}$$

$$q_{s|t}(x_s^i|\mathbf{x}_t) = \begin{cases} 1, & x_t^i \neq [m], x_s^i = x_t^i, \\ \frac{1 - \alpha_s}{1 - \alpha_t}, & x_t^i = [m], x_s^i = [m], \\ \frac{\alpha_s - \alpha_t}{1 - \alpha_t} q_{0|t}(x_s^i|\mathbf{x}_t), & x_t^i = [m], x_s^i \neq [m], \\ 0, & \text{otherwise.} \end{cases} \quad (2)$$

In MDM, a parameterized reverse model p_θ is often employed to approximate the distribution $q_{0|t}(x_s^i|\mathbf{x}_t)$. This model is trained by minimizing the evidence lower bound (ELBO) (Lou et al., 2024; Shi et al., 2024; Gong et al., 2024; Sahoo et al., 2024) on the negative log-likelihood of the data distribution q_0 .

Inference. Inference within the MDM framework entails discretizing the reverse process to iteratively reconstruct

sequences from a fully masked sequence. Let T denote the number of sampling steps. Starting with a fully masked sequence, the denoising process proceeds via $q_{s|t}(\mathbf{x}_s|\mathbf{x}_t)$, where $s = \frac{i}{T}$ and $t = \frac{i+1}{T}$. At each step, the model first samples \mathbf{x}_0 from the conditional distribution $p_\theta(\mathbf{x}_0|\mathbf{x}_t)$, followed by masking specific tokens according to $q(\mathbf{x}_s|\mathbf{x}_t, \mathbf{x}_0)$.

In practice, the reverse model is parameterized using a factorized denoising model, where the conditional distribution $p_\theta(\mathbf{x}_0|\mathbf{x}_t)$ is expressed as:

$$p_\theta(\mathbf{x}_0|\mathbf{x}_t) = \prod_{i=1}^L p_\theta(x_0^i|\mathbf{x}_t). \quad (3)$$

Here, each token is predicted independently using $p_\theta(x_0^i|\mathbf{x}_t)$, allowing for efficient parallel sampling. However, this factorized approach imposes a significant limitation: it disregards interdependencies between tokens within the sequence. As a result, the factorized model $p_\theta(\mathbf{x}_0|\mathbf{x}_t)$ cannot exactly match the true reverse distribution $q(\mathbf{x}_0|\mathbf{x}_t)$ (Xu et al., 2024). In this work, we analyze the conditions under which this sampling method achieves a favorable balance between efficiency and the quality of the generated sequences.

4. Theoretical Analysis

In image generation, the primary goal is typically to produce visually appealing and seamless images (Heusel et al., 2017). Language generation is more task-specific. Depending on the application, the users may prefer fluent outputs, as in article writing, or precise and accurate reasonings, as in problem-solving tasks. In this section, we explore the sampling efficiency of MDMs in addressing various language tasks with respect to different evaluation metrics.

4.1. Notations and Problem Setting

Our investigation employs the hidden Markov model (HMM) framework to analyze natural language generation. This section establishes the formal notation and problem setting that underlies our subsequent analysis.

HMMs (Eddy, 1996) provide a probabilistic foundation for modeling sequential data with latent structures, where observed sequences are generated by an underlying sequence of unobservable hidden states. Formally, an HMM $\mathcal{H} = (\mathcal{S}, \mathcal{V}, \mathbf{A}, \mathbf{B})$ is characterized by the following components: a finite set of hidden states $\mathcal{S} = \{s_1, s_2, \dots, s_N\}$, an observable vocabulary \mathcal{V} , a state transition probability matrix $\mathbf{A} \in \mathbb{R}^{N \times N}$, an emission probability matrix $\mathbf{B} \in \mathbb{R}^{N \times |\mathcal{V}|}$, and an initial state distribution $\boldsymbol{\pi} \in \mathbb{R}^N$. Given a sequence of observations $\mathbf{x} = (x_1, x_2, \dots, x_L) \in \mathcal{V}^L$ and a sequence of hidden states $\mathbf{s} = (s_1, s_2, \dots, s_L) \in \mathcal{S}^L$, the generative process of an HMM is governed by the following probabilis-

tic relations:

$$\Pr(s_1) = \pi_{s_1}, \quad \Pr(x_i | s_i) = B_{s_i, x_i},$$

$$\Pr(s_i | s_{1:i-1}) = \Pr(s_i | s_{i-1}) = A_{s_{i-1}, s_i}.$$

This formulation enables HMMs to capture both the sequential dependencies among hidden states and their probabilistic relationships with observed data. In the field of NLP, HMMs serve as the fundamental statistical tools to model natural language (Eddy, 1996; Marti & Bunke, 2001). A notable special case of HMM is the n -gram language model (Brown et al., 1992), which estimates the probability of a token given its preceding $n - 1$ tokens. Despite their simplicity, n -gram models are foundational tools in NLP tasks (Brown et al., 1992; De Novais et al., 2010). Moreover, Liu et al. (2024) suggests that scaling up n -gram models can also achieve performance comparable to modern large language models.

Formally, we aim to address the following question: If MDMs have the capability to approximate a target HMM model, what are the computational costs, and do MDMs offer advantages over auto-regressive models? To evaluate the approximation quality of MDMs, we adopt two widely used metrics: *TER* and *SER*, which quantify different aspects of a model’s performance.

Token Error Rate. In practice, perplexity is one of the most widely used metrics for evaluating token-level errors in language models. It quantifies the uncertainty of a model in predicting the next token in a sequence and serves as a standard measure for assessing the quality of text generation. In this paper, we define the TER by perplexity. Models with lower TER are generally considered more effective at generating fluent and coherent text. Formally, given a ground-truth language model q and an evaluated model p , the TER is computed as:

$$\text{TER}(p) = 2^{\mathbb{E}_{\mathbf{x} \sim q} \left[-\frac{\log(p(\mathbf{x}))}{|\mathbf{x}|} \right]}. \quad (4)$$

Sequence Error Rate. The SER evaluates the correctness of an entire sequence rather than individual tokens. Let q represent a target language defined over a vocabulary \mathcal{V} , and let $\mathcal{L}_q = \{\mathbf{x} \in \mathcal{V}^* \mid q(\mathbf{x}) > 0\}$ denote the support set of distribution q . For a generative model p , the SER is defined as:

$$\text{SER}(p) = 1 - \sum_{\mathbf{x} \in \mathcal{L}_q} p(\mathbf{x}). \quad (5)$$

This metric quantifies the probability that the model generates sequences falling outside the support set of the ground-truth distribution.

Compared to TER, SER imposes a stricter evaluation criterion by requiring the correctness of entire sequences. This makes SER particularly well-suited for tasks that demand logical consistency or reasoning, where the correctness of the complete reasoning chain is crucial.

4.2. MDMs Can Generate Low-TER Sentences Efficiently

In this subsection, we rigorously examine the efficiency of sampling in MDMs, demonstrating that MDMs are capable of efficiently generating sentences with near-optimal TER. To establish the main theoretical results, we assume that the MDMs have enough expressive power and begin with the following assumption:

Assumption 4.1 (Learning with Small Error). Let q denote the target language model with vocabulary \mathcal{V} , and let p_θ represent the reverse model trained to approximate the reverse process generating the target language under a masking schedule α_t . Assume there exists $\epsilon_{\text{learning}} > 0$ such that the KL divergence between p_θ and the reverse process distribution generating the language q is bounded by $\epsilon_{\text{learning}}$, i.e.,

$$D_{\text{KL}}(q_{0|t}(x_0^i | \mathbf{x}_t) \| p_\theta(x_0^i | \mathbf{x}_t)) < \epsilon_{\text{learning}}, \quad \forall t \text{ and } \mathbf{x}_t.$$

It is worth noting that $p_\theta(x_0^i | \mathbf{x}_t) = q_{0|t}(x_0^i | \mathbf{x}_t)$ represents the optimal solution to the ELBO loss during training. Assumption 4.1 implies that the MDM model is well-trained and approximates the ground-truth distribution with only a small error.

During MDM inference, the time interval $[0, 1]$ is discretized into N steps, where $t_i = \frac{i}{N}$, $i \in [N]$, and iteratively reconstruct sequences from a fully masked sequence. The following theorem shows that the sequence distribution generated by the reverse process, even with a small number of sampling steps, can achieve near-optimal TER. Consequently, MDMs exhibit high efficiency in generating n -gram language.

Theorem 4.2 (TER Bounds for n -Gram Language Generation). For any n -gram language q and any $\epsilon > 0$, let p_θ denote the reverse model and L denote the sequence length. The distribution over sequences generated by p_θ is denoted as p . For any $L > O\left(\frac{n-1}{\epsilon^{n+0.5}}\right)$, under Assumption 4.1, there exists a masking schedule α_t such that, with $N = O\left(\frac{n-1}{\epsilon^n}\right)$ sampling steps, the TER of the MDM is upper-bounded by:

$$\log \text{TER}(p) \leq \log \text{TER}(q) + \epsilon_{\text{learning}} + 4\epsilon \log |\mathcal{V}|. \quad (6)$$

The proof of this theorem is presented in Appendix B.

Theorem 4.2 demonstrates that MDMs can efficiently generate sentences with high fidelity. It is notable that for a given data distribution q , the TER of a language model p achieves its global minimum when $p = q$. To ensure a gap of at most ϵ with the optimal TER during sampling, the number of required sampling steps is bounded by $O\left(\frac{n-1}{\epsilon^n}\right)$.

The above results suggest that to achieve near-optimal TER, MDMs require only a number of sampling steps that is

independent of the sequence length L . In each sampling step, the neural network model, i.e., a Transformer, is executed once. Therefore, informally, the neural network execution count is constant for MDM. This offers substantial efficiency gains over auto-regressive models, where the model must be executed L times, once for each token in the sequence. Such efficiency enables MDMs to handle long-sequence generation tasks effectively while maintaining high-quality outputs.

4.3. MDMs Cannot Generate Low-SER Sentences with A Low Cost

In this subsection, we examine the SER of sampling in MDMs and highlight a fundamental limitation of MDMs in generating logically rigorous language. We begin by establishing that, with sufficient sampling steps, the MDMs have the capability to approximate a target HMM model with perfect SER.

Theorem 4.3 (Accurate Generation of HMM with Sufficient Steps). *Let q denote any HMM, and let p_θ represent the reverse model under an arbitrary masking schedule, where L is the sequence length. Let p denote the distribution over sequences generated by p_θ . Under Assumption 4.1 with a learning error $\epsilon_{\text{learning}} < O(\frac{\delta}{L})$, and given a sufficient number of reverse steps, the sequence error rate $\text{SER}(p)$ of the generated text satisfies*

$$\text{SER}(p) \leq \delta.$$

The complete proof of Theorem 4.3 is detailed in Appendix C.1. While this result establishes the theoretical capability of MDMs to achieve low SER, we still need to estimate the computational cost to achieve it. The following theorem provides a negative result for this problem.

Theorem 4.4 (SER Bound for HMM Generation). *There exists an HMM q over a vocabulary of size 16 that satisfies the following conditions: for any reverse model p_θ under Assumption 4.1 with $\epsilon_{\text{learning}} < \frac{1}{128}$, and any masking schedule α_t , let p denote the distribution over sequences generated by p_θ . There exists a constant C such that if the number of sampling steps satisfies $N = CL$, where L is the sequence length, the SER of the generated text is lower-bounded by:*

$$\text{SER}(p) > \frac{1}{2}.$$

The proof is presented in Appendix C.2.

Theorem 4.4 shows that to generate sequences with low SER, the number of sampling steps in MDMs must scale at least linearly with the sequence length L , indicating that the number of neural network executions is comparable between MDMs and autoregressive models. However, this scaling

law of MDMs typically leads to much higher computational costs compared to autoregressive models. For instance, in the case of Transformer-based architectures, each execution step in MDMs involves a quadratic computational complexity in terms of L , as opposed to the linear complexity of auto-regressive Transformer models in each generation step (through reusing the stored KV caches). Consequently, in accuracy-critical applications, MDMs offer no computational efficiency advantage over auto-regressive models.

Furthermore, some prior works (Sahoo et al., 2024; Ou et al., 2024) have proposed efficient sampling strategies that reuse cached outputs without requiring additional forward passes through the network when no token is modified from $[m]$ at a given step. Nevertheless, our theoretical results remain applicable to these sampling strategies, as discussed in Appendix D.

Do TER and SER Conflict? The above results reveal that MDMs can efficiently generate low-TER sentences but may incur higher costs when evaluating the generation under SER. One might think these results are contradictory. Note that several previous works have already shown that TER (a.k.a perplexity) may not reflect a model’s true performance in solving several long-sequence understanding tasks (Huang et al., 2022; Hu et al., 2024; Luden et al., 2024). Thus, it is natural to arrive at different conclusions depending on the metric used.

Moreover, many practical scenarios have shown that the choice of evaluation metric significantly influences the conclusion of other problems. For instance, while the community has previously focused on the emergence phenomenon, recent works by Wei et al. (2022a) and Schaeffer et al. (2024) demonstrate that this phenomenon may stem from the use of non-smooth evaluation metrics. Our work further reveals that conclusions regarding the efficiency of MDMs depend heavily on the evaluation metric employed. Specifically, MDMs excel in applications where fluency is prioritized. In contrast, for reasoning-intensive tasks that demand highly accurate trajectories, MDMs may fail to offer a significant efficiency advantage over auto-regressive models.

5. Experiments

We conducted a series of experiments to empirically validate the theoretical findings, focusing on evaluating the sampling quality and computational efficiency of MDMs under diverse metrics. The results reveal that while MDMs effectively generate low-TER sequences, but achieving low-SER demands substantial computational resources. We will first introduce our experimental settings and then present the experimental results.

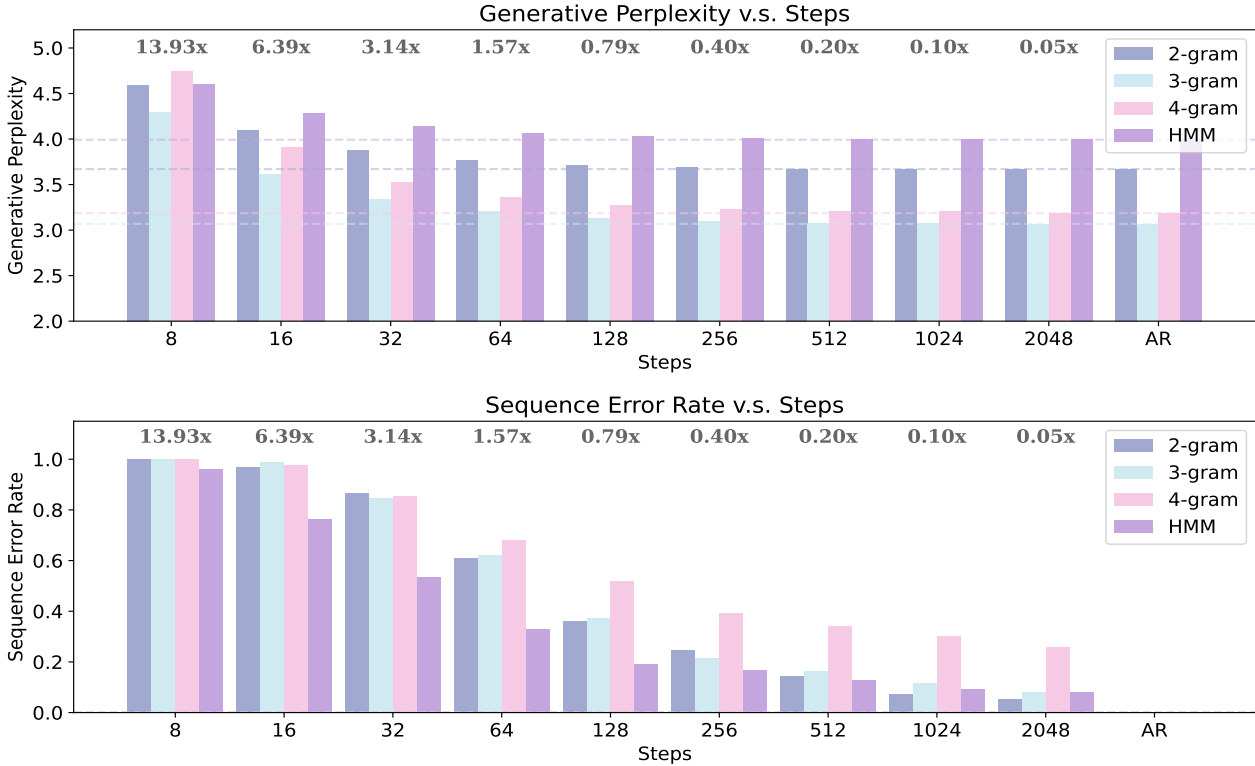


Figure 1. Sampling Efficiency and Quality of MDMs on Formal Languages: The above subfigure illustrates generative perplexity of generated sequences versus the number of sampling steps for n -gram languages ($n \in \{2, 3, 4\}$) and HMM. The y-axis represents the generative perplexity, and the x-axis represents the sampling steps, with the last point indicating the performance of auto-regressive models. The figure below shows the SER of generated sequences versus the number of sampling steps for the same formal languages. The y-axis represents the SER, while the x-axis is the same as the above figure. The number above each bar indicates the speedup of MDMs under different sampling steps compared to the auto-regressive models.

5.1. Experimental Setup

Tasks and Datasets. First, we evaluated MDMs on a variety of formal languages, including n -gram languages ($n \in \{2, 3, 4\}$) and HMMs. For each formal language, parameters such as transition matrices, observation matrices, and initial distributions were generated through random sampling. Detailed descriptions of the parameter generation process, along with illustrative examples of the resulting sequences, are provided in Appendix E.1. Using these formal languages, we constructed datasets comprising 1,000,000 samples, of which 990,000 were allocated for training and 10,000 for validation. When using the formal language models to generate the dataset, we set the max length of 512.

Model Training. We adopted transformer-based architectures as the backbone models due to their scalability and expressiveness in sequence modeling tasks. Comprehensive architectural details, including the number of layers, hidden dimensions, and positional encoding schemes, are provided in Table 2 in Appendix E.2. The training process followed the framework proposed by Sahoo et al. (2024), with additional training configurations detailed in Table 3. Models were trained for 20 epochs, and their convergence was monitored using the validation set. Perplexity was used

as the primary convergence metric, and the trained models achieved optimal perplexity values consistent with the ground-truth language models that generated the datasets.

Evaluation Metrics. To assess the quality of generated sequences, we used TER and SER as the primary evaluation metrics, in alignment with our theoretical framework. Computational efficiency was evaluated based on the number of sampling steps. Following prior work (Lou et al., 2024; Xu et al., 2024), generative perplexity was employed as the TER metric to evaluate the sample qualities under different sampling steps. We compute the generative perplexity using the ground-truth model to evaluate the likelihood of sequences generated by MDMs, which were subsequently converted into perplexity scores. SER was computed directly using its definition in Equation (5), leveraging ground-truth models for evaluation. For sequence generation, we utilized the `ddpm_cache` sampler proposed in prior work (Sahoo et al., 2024), ensuring efficient sampling. Computational efficiency was measured by the number of sampling steps, and we further discuss the influence of `ddpm_cache` under different sampling steps in Appendix D. Furthermore, we also test the true speedup of MDMs under different sampling steps compared

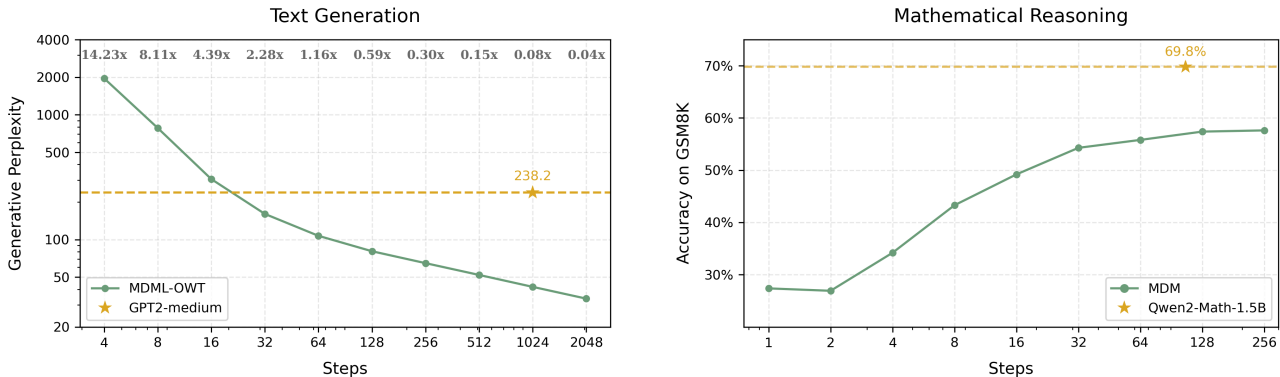


Figure 2. Evaluation on Language Tasks: The left subfigure illustrates the text generation quality of MDLM-OWT across different sampling steps, with GPT2-medium as baseline. The y-axis represents the average generative perplexity of 2000 generated texts, and the x-axis indicates the number of sampling steps. The numbers above indicate the speedup of MDLM-OWT under different sampling steps compared to GPT2-medium. The right subfigure shows the accuracy of MDM on the GSM8K benchmark at different sampling steps, with Qwen-Math-1.5B as baseline. The y-axis indicates accuracy, and the x-axis represents the number of sampling steps.

to the auto-regressive models in Figure 1, the detailed testing settings are listed in Appendix E.2. To ensure robust evaluation, we generated 2000 sequences for each setting and computed both TER and SER over these samples.

To compare MDMs with auto-regressive models, we trained auto-regressive models with identical architectures and model sizes on the same datasets generated by the formal languages. These models were evaluated under the same metrics, serving as a baseline for performance comparison. The training configurations are provided in Table 4.

5.2. Experiment Results

The experiment results are presented in Figure 1. The upper subfigure shows the generative perplexity across different formal languages with the number of sampling steps varying. The x-axis represents the number of sampling steps, ranging from 8 to 2048, while the y-axis measures the generative perplexity, where lower values indicate higher text fluency and token-level accuracy. The performance of auto-regressive models is marked as the final point on the x-axis for comparison. As shown in the figure, MDMs achieve near-optimal generative perplexity with relatively few sampling steps. To achieve a perplexity similar to the auto-regressive model, MDMs only require about 64 steps and demonstrate 1.57 times speedup compared to auto-regressive models. This demonstrates that MDMs are highly efficient at generating fluent sequences even with a small number of sampling steps. As the number of sampling steps increases, the performance of MDMs approaches that of auto-regressive models, converging to a similar level of generative perplexity.

The lower subfigure evaluates the relationship between the number of sampling steps and the SER, which measures the correctness of an entire sequence. The x-axis again represents the number of sampling steps, with the performance of auto-regressive models included as a baseline, and

the y-axis measures the SER, where lower values indicate higher sequence-level accuracy. Compared to the upper subfigure, this subfigure reveals a slower improvement in SER as the number of sampling steps increases. For these formal languages, achieving low SER requires significantly more sampling steps. Moreover, even when the number of sampling steps reaches 2048, there remains a gap in SER between MDMs and auto-regressive models. These results demonstrate that auto-regressive models maintain a clear advantage in SER, as their token-by-token generation achieves zero SER across these tasks.

Figure 1 highlights the trade-off between efficiency and accuracy for MDMs empirically. While MDMs excel in generating fluent outputs with low TER, they require substantially more sampling steps to achieve low SER, particularly for reasoning-intensive tasks that demand sequence-level correctness. These experimental results further reinforce our theoretical findings.

6. Preliminary Experiments on Large Models

We further conducted an extensive set of experiments on language tasks using open-source MDMs. First, we evaluated the quality of text generation by measuring the generative perplexity of MDMs using MDLM-OWT (Sahoo et al., 2024), a diffusion language model trained on OpenWebText (Gokaslan & Cohen, 2019). For a fair comparison, we evaluated GPT2-medium (Radford et al., 2019), which is similar in size. Second, we explored the mathematical reasoning ability of MDMs on the GSM8K dataset (Cobbe et al., 2021). Given that small models typically exhibit poor reasoning performance, we used a fine-tuned diffusion language model with 1.1B non-embedding parameters proposed by Nie et al. (2024), and compared it against model with a similar number of parameters. While the generative perplexity represents the metric of TER, mathematical rea-

soning is more concerned with the correctness of the entire generated sequence, thus, the GSM8K accuracy is partially consistent with the negative sequence error rate – SER.

Text Generation. For text generation, we use MDLM-OWT, which has a context length of 1024 and size similar to GPT2-medium and is trained on OWT dataset (Gokaslan & Cohen, 2019). Since our goal is to compare the acceleration of MDMs relative to auto-regressive models and examine the effect of the number of steps on text generation quality, the absolute size and capability of the model are less important. Following the approach in the original work, we used the `ddpm_cache` sampler and the GPT2 tokenizer. For the number of sampling steps ranging from 4 to 2048, we generated 2000 samples of length 1024 and evaluated the generative perplexity using GPT2-large. To compare MDMs with auto-regressive models, we took GPT2-medium as baseline and computed its generative perplexity in the same manner.

The experiment result is shown in the left subfigure of Figure 2, which illustrates the text generation quality of MDLM-OWT across different sampling steps, with GPT2-medium as the baseline. The x-axis represents the number of sampling steps, and the y-axis represents the average generative perplexity of 2000 generated texts, where lower generative perplexity indicates higher fluency and, consequently, a lower TER. The numbers above indicate the speedup of MDLM-OWT under different sampling steps compared to GPT2-medium. As is shown in the figure, MDLM-OWT matches the generative perplexity of GPT2-medium with only 32 steps, where there is a 2.28x speedup, and the perplexity continues to decline and converge as the number of sampling steps increases. This demonstrates that MDMs can generate texts efficiently while ensuring a high fluency, which illustrates the potential of MDMs for basic language generation tasks at a larger scale.

Mathematical Reasoning. For mathematical reasoning, we used the MDM provided by Nie et al. (2024), which was fine-tuned on GSM8K using a model trained on SlimPajama (Soboleva et al., 2023) for 3.3×10^{21} training FLOPs with 1.1B non-embedding parameters. This is so far the first MDM to be fine-tuned on mathematical reasoning tasks. We generated answers with a maximum length of 256 for the number of sampling steps ranging from 1 to 256. Since there are very few models fine-tuned on GSM8K at the same scale, we took Qwen2-Math-1.5B (Yang et al., 2024) as our baseline. We evaluated its performance following the widely used Language Model Evaluation Harness framework (Gao et al., 2024), and counted the average length of the generated answers, which partly reflects the efficiency of the model.

The experiment results are presented in the right subfigure of Figure 2. For all tested step numbers, the average length of generated answers for MDM is around 30, while for the baseline model, the average length is about 105. Unlike text

generation, MDM does not show a significant advantage over auto-regressive models for mathematical reasoning tasks. The accuracy of the MDM decreases sharply as the number of steps falls below the sequence length, and it shows only a slight improvement as the number of samples exceeds the sequence length. While the latter may be due to the limitations of the MDM we used, the former likely caused by insufficient sampling, which leads to a high sequence error rate. It is worth noting that the experimental setup for the MDM differs from that of the baseline models, so the baseline accuracy is provided only for reference.

Summary. Figure 2 illustrates the performance of MDMs on language tasks and its dependence on sampling steps. For text generation, MDLM-OWT achieved similar performance to GPT2-medium with few sampling steps, demonstrating efficiency in generating fluent text. On the contrary, MDMs showed no significant advantage on the GSM8K accuracy, with performance declining rapidly when the number of steps fell below the sequence length. These results highlight MDMs’ ability in text generation, but suggest challenges in reasoning-relevant tasks.

7. Conclusion and Limitations

Conclusion. This paper provides a rigorous theoretical and empirical analysis of the efficiency of MDMs under various metrics. We demonstrate that MDMs can achieve near-optimal TER with a fixed number of sampling steps, regardless of sequence length, making them highly efficient for tasks emphasizing fluency. However, when evaluated using SER, MDMs require sampling steps that scale linearly with sequence length, negating their efficiency advantage over auto-regressive models. These findings highlight the trade-off between efficiency and accuracy, depending on the evaluation metric. Experimental results further reinforce our theoretical results across formal and natural language tasks, offering practical guidance for deploying MDMs. While MDMs demonstrate efficiency advantages in applications prioritizing fluency, they may fall short in reasoning-intensive tasks requiring high accuracy compared to auto-regressive models.

Limitations. Our study focuses on formal languages modeled using HMM, which, while foundational, still differs from modern language models. Extending this analysis to more advanced language models remains an important direction for future work. Additionally, we primarily analyze Masked Diffusion Models, but the broader family of diffusion-based language models, including variants like SEDD-uniform (Lou et al., 2024), requires further investigation. In summary, while our work establishes a theoretical understanding of MDMs, further exploration is needed to generalize our findings to real-world settings and to systematically analyze other diffusion approaches.

Impact Statement

This paper presents work whose goal is to advance the field of generative models. There are many potential societal consequences of our work, none of which we feel must be specifically highlighted here.

References

- Achiam, J., Adler, S., Agarwal, S., Ahmad, L., Akkaya, I., Aleman, F. L., Almeida, D., Altenschmidt, J., Altman, S., Anadkat, S., et al. Gpt-4 technical report. *arXiv preprint arXiv:2303.08774*, 2023.
- Austin, J., Johnson, D. D., Ho, J., Tarlow, D., and van den Berg, R. Structured denoising diffusion models in discrete state-spaces. In *Advances in Neural Information Processing Systems*, 2021.
- Avdeyev, P., Shi, C., Tan, Y., Dudnyk, K., and Zhou, J. Dirichlet diffusion score model for biological sequence generation. In *International Conference on Machine Learning*, pp. 1276–1301. PMLR, 2023.
- Bahdanau, D. Neural machine translation by jointly learning to align and translate. *arXiv preprint arXiv:1409.0473*, 2014.
- Brown, P. F., Della Pietra, V. J., Desouza, P. V., Lai, J. C., and Mercer, R. L. Class-based n-gram models of natural language. *Computational linguistics*, 18(4):467–480, 1992.
- Bubeck, S., Chandrasekaran, V., Eldan, R., Gehrke, J., Horvitz, E., Kamar, E., Lee, P., Lee, Y. T., Li, Y., Lundberg, S., et al. Sparks of artificial general intelligence: Early experiments with gpt-4. *arXiv preprint arXiv:2303.12712*, 2023.
- Campbell, A., Benton, J., Bortoli, V. D., Rainforth, T., Deligiannidis, G., and Doucet, A. A continuous time framework for discrete denoising models. In *Advances in Neural Information Processing Systems*, 2022.
- Campbell, A., Yim, J., Barzilay, R., Rainforth, T., and Jaakkola, T. Generative flows on discrete state-spaces: Enabling multimodal flows with applications to protein co-design. In *Forty-first International Conference on Machine Learning*, 2024. URL <https://openreview.net/forum?id=kQwSbv0BR4>.
- Chen, T., Zhang, R., and Hinton, G. Analog bits: Generating discrete data using diffusion models with self-conditioning. *arXiv preprint arXiv:2208.04202*, 2022.
- Cobbe, K., Kosaraju, V., Bavarian, M., Chen, M., Jun, H., Kaiser, L., Plappert, M., Tworek, J., Hilton, J., Nakano, R., Hesse, C., and Schulman, J. Training verifiers to solve math word problems. *arXiv preprint arXiv:2110.14168*, 2021.
- Dai, Z. Transformer-xl: Attentive language models beyond a fixed-length context. *arXiv preprint arXiv:1901.02860*, 2019.
- Davis, O., Kessler, S., Petrache, M., Ceylan, I. I., Bronstein, M., and Bose, A. J. Fisher flow matching for generative modeling over discrete data. *arXiv preprint arXiv:2405.14664*, 2024.
- De Novais, E. M., Dias Tadeu, T., and Paraboni, I. Improved text generation using n-gram statistics. In *Advances in Artificial Intelligence—IBERAMIA 2010: 12th Ibero-American Conference on AI, Bahía Blanca, Argentina, November 1-5, 2010. Proceedings 12*, pp. 316–325. Springer, 2010.
- Devlin, J., Chang, M.-W., Lee, K., and Toutanova, K. BERT: Pre-training of deep bidirectional transformers for language understanding. In *Proceedings of the 2019 Conference of the North American Chapter of the Association for Computational Linguistics: Human Language Technologies, Volume 1 (Long and Short Papers)*. Association for Computational Linguistics, 2019.
- Dieleman, S., Sartran, L., Roshannai, A., Savinov, N., Ganin, Y., Richemond, P. H., Doucet, A., Strudel, R., Dyer, C., Durkan, C., Hawthorne, C., Leblond, R., Grathwohl, W., and Adler, J. Continuous diffusion for categorical data. *ArXiv*, abs/2211.15089, 2022.
- Eddy, S. R. Hidden markov models. *Current opinion in structural biology*, 6(3):361–365, 1996.
- Floridi, L. and Chiriatti, M. Gpt-3: Its nature, scope, limits, and consequences. *Minds and Machines*, 30:681–694, 2020.
- Gao, L., Tow, J., Abbasi, B., Biderman, S., Black, S., DiPofi, A., Foster, C., Golding, L., Hsu, J., Le Noac’h, A., Li, H., McDonell, K., Muennighoff, N., Ociepa, C., Phang, J., Reynolds, L., Schoelkopf, H., Skowron, A., Sutawika, L., Tang, E., Thite, A., Wang, B., Wang, K., and Zou, A. A framework for few-shot language model evaluation, 07 2024. URL <https://zenodo.org/records/12608602>.
- Gat, I., Remez, T., Shaul, N., Kreuk, F., Chen, R. T., Synnaeve, G., Adi, Y., and Lipman, Y. Discrete flow matching. *arXiv preprint arXiv:2407.15595*, 2024.
- Gokaslan, A. and Cohen, V. Openwebtext corpus. <http://Skylion007.github.io/OpenWebTextCorpus>, 2019.

- Gong, S., Agarwal, S., Zhang, Y., Ye, J., Zheng, L., Li, M., An, C., Zhao, P., Bi, W., Han, J., et al. Scaling diffusion language models via adaptation from autoregressive models. *arXiv preprint arXiv:2410.17891*, 2024.
- Gulrajani, I. and Hashimoto, T. Likelihood-based diffusion language models. In *Advances in Neural Information Processing Systems*, 2023.
- He, Z., Sun, T., Wang, K., Huang, X., and Qiu, X. Diffusion-bert: Improving generative masked language models with diffusion models. In *Annual Meeting of the Association for Computational Linguistics*, 2022.
- Heusel, M., Ramsauer, H., Unterthiner, T., Nessler, B., and Hochreiter, S. Gans trained by a two time-scale update rule converge to a local nash equilibrium. *Advances in neural information processing systems*, 30, 2017.
- Ho, J., Jain, A., and Abbeel, P. Denoising diffusion probabilistic models. In *Advances in Neural Information Processing Systems*, 2020.
- Hu, Y., Huang, Q., Tao, M., Zhang, C., and Feng, Y. Can perplexity reflect large language model’s ability in long text understanding?, 2024. URL <https://arxiv.org/abs/2405.06105>.
- Huang, F., Tao, T., Zhou, H., Li, L., and Huang, M. On the learning of non-autoregressive transformers. *ArXiv*, abs/2206.05975, 2022. URL <https://api.semanticscholar.org/CorpusID:249626415>.
- Jelinek, F., Mercer, R. L., Bahl, L. R., and Baker, J. K. Perplexity—a measure of the difficulty of speech recognition tasks. *The Journal of the Acoustical Society of America*, 62(S1):S63–S63, 1977.
- Karras, T., Aittala, M., Aila, T., and Laine, S. Elucidating the design space of diffusion-based generative models. In *Advances in Neural Information Processing Systems*, 2022.
- Leviathan, Y., Kalman, M., and Matias, Y. Fast inference from transformers via speculative decoding. In *International Conference on Machine Learning*, pp. 19274–19286. PMLR, 2023.
- Lin, C.-Y. Rouge: A package for automatic evaluation of summaries. In *Text summarization branches out*, pp. 74–81, 2004.
- Liu, J., Min, S., Zettlemoyer, L., Choi, Y., and Hajishirzi, H. Infini-gram: Scaling unbounded n-gram language models to a trillion tokens. *arXiv preprint arXiv:2401.17377*, 2024.
- Lou, A., Meng, C., and Ermon, S. Discrete diffusion modeling by estimating the ratios of the data distribution. In *Proceedings of the 41st International Conference on Machine Learning*, pp. 32819–32848. PMLR, 2024.
- Lovelace, J., Kishore, V., Chen, Y., and Weinberger, K. Q. Diffusion guided language modeling. *arXiv preprint arXiv:2408.04220*, 2024.
- Luden, I., Giulianelli, M., and Fernández, R. Beyond perplexity: Examining temporal generalization in large language models via definition generation. *Computational Linguistics in the Netherlands Journal*, 13:205–232, 2024.
- Marti, U.-V. and Bunke, H. Using a statistical language model to improve the performance of an hmm-based cursive handwriting recognition system. *International journal of Pattern Recognition and Artificial intelligence*, 15(01):65–90, 2001.
- Meng, C., Choi, K., Song, J., and Ermon, S. Concrete score matching: Generalized score matching for discrete data. In *Advances in Neural Information Processing Systems*, 2022.
- Nie, S., Zhu, F., Du, C., Pang, T., Liu, Q., Zeng, G., Lin, M., and Li, C. Scaling up masked diffusion models on text. *arXiv preprint arXiv:2410.18514*, 2024.
- Ou, J., Nie, S., Xue, K., Zhu, F., Sun, J., Li, Z., and Li, C. Your absorbing discrete diffusion secretly models the conditional distributions of clean data. *arXiv preprint arXiv:2406.03736*, 2024.
- Ouyang, S., Zhang, J. M., Harman, M., and Wang, M. Llm is like a box of chocolates: the non-determinism of chatgpt in code generation. *arXiv preprint arXiv:2308.02828*, 2023.
- Papineni, K., Roukos, S., Ward, T., and Zhu, W.-J. Bleu: a method for automatic evaluation of machine translation. In *Proceedings of the 40th annual meeting of the Association for Computational Linguistics*, pp. 311–318, 2002.
- Radford, A., Wu, J., Child, R., Luan, D., Amodei, D., Sutskever, I., et al. Language models are unsupervised multitask learners. *OpenAI blog*, 1(8):9, 2019.
- Rastogi, R., Schiff, Y., Hacothen, A., Li, Z., Lee, I., Deng, Y., Sabuncu, M. R., and Kuleshov, V. Semi-parametric inducing point networks and neural processes. *arXiv preprint arXiv:2205.11718*, 2022.
- Roziere, B., Gehring, J., Gloeckle, F., Sootla, S., Gat, I., Ellen, X., Adi, Y., Liu, J., Sauvestre, R., Remez, T., et al. Code llama: Open foundation models for code. *arXiv preprint arXiv:2308.12950*, 2023.

- Sahoo, S. S., Arriola, M., Schiff, Y., Gokaslan, A., Marroquin, E., Chiu, J. T., Rush, A., and Kuleshov, V. Simple and effective masked diffusion language models, 2024.
- Schaeffer, R., Miranda, B., and Koyejo, S. Are emergent abilities of large language models a mirage? *Advances in Neural Information Processing Systems*, 36, 2024.
- Shi, J., Han, K., Wang, Z., Doucet, A., and Titsias, M. K. Simplified and generalized masked diffusion for discrete data. *arXiv preprint arXiv:2406.04329*, 2024.
- Soboleva, D., Al-Khateeb, F., Myers, R., Steeves, J. R., Hestness, J., and Dey, N. SlimPajama: A 627B token cleaned and deduplicated version of RedPajama, 06 2023. URL <https://huggingface.co/datasets/cerebras/SlimPajama-627B>.
- Sohl-Dickstein, J., Weiss, E., Maheswaranathan, N., and Ganguli, S. Deep unsupervised learning using nonequilibrium thermodynamics. In *Proceedings of the 32nd International Conference on Machine Learning*, 2015.
- Song, J., Meng, C., and Ermon, S. Denoising diffusion implicit models. In *International Conference on Learning Representations*, 2021a. URL <https://openreview.net/forum?id=StlgIarCHLP>.
- Song, Y., Sohl-Dickstein, J., Kingma, D. P., Kumar, A., Ermon, S., and Poole, B. Score-based generative modeling through stochastic differential equations. In *International Conference on Learning Representations*, 2021b. URL <https://openreview.net/forum?id=PxTIG12RRHS>.
- Sun, Z. and Yang, Y. Difusco: Graph-based diffusion solvers for combinatorial optimization. *Advances in Neural Information Processing Systems*, 36:3706–3731, 2023.
- Sutskever, I. Sequence to sequence learning with neural networks. *arXiv preprint arXiv:1409.3215*, 2014.
- Vignac, C., Krawczuk, I., Siraudin, A., Wang, B., Cevher, V., and Frossard, P. Digress: Discrete denoising diffusion for graph generation. *arXiv preprint arXiv:2209.14734*, 2022.
- Wei, J., Tay, Y., Bommasani, R., Raffel, C., Zoph, B., Borgeaud, S., Yogatama, D., Bosma, M., Zhou, D., Metzler, D., et al. Emergent abilities of large language models. *Transactions on Machine Learning Research*, 2022a.
- Wei, J., Wang, X., Schuurmans, D., Bosma, M., Xia, F., Chi, E., Le, Q. V., Zhou, D., et al. Chain-of-thought prompting elicits reasoning in large language models. *Advances in neural information processing systems*, 35:24824–24837, 2022b.
- Wu, Y., Schuster, M., Chen, Z., Le, Q. V., Norouzi, M., Macherey, W., Krikun, M., Cao, Y., Gao, Q., Macherey, K., et al. Google’s neural machine translation system: Bridging the gap between human and machine translation. *arXiv preprint arXiv:1609.08144*, 2016.
- Xu, M., Geffner, T., Kreis, K., Nie, W., Xu, Y., Leskovec, J., Ermon, S., and Vahdat, A. Energy-based diffusion language models for text generation. *arXiv preprint arXiv:2410.21357*, 2024.
- Yang, A., Yang, B., Hui, B., Zheng, B., Yu, B., Zhou, C., Li, C., Li, C., Liu, D., Huang, F., et al. Qwen2 technical report. *arXiv preprint arXiv:2407.10671*, 2024.
- Ye, J., Zheng, Z., Bao, Y., Qian, L., and Gu, Q. Diffusion language models can perform many tasks with scaling and instruction-finetuning. *arXiv preprint arXiv:2308.12219*, 2023.
- Zhang, H., Dang, M., Peng, N., and Van den Broeck, G. Tractable control for autoregressive language generation. In *International Conference on Machine Learning*, pp. 40932–40945. PMLR, 2023.
- Zhang, S., Wu, L., Gong, C., and Liu, X. Language rectified flow: Advancing diffusion language generation with probabilistic flows. *arXiv preprint arXiv:2403.16995*, 2024.
- Zhao, L., Ding, X., Yu, L., and Akoglu, L. Improving and unifying discrete&continuous-time discrete denoising diffusion. *arXiv preprint arXiv:2402.03701*, 2024.
- Zheng, K., Chen, Y., Mao, H., Liu, M.-Y., Zhu, J., and Zhang, Q. Masked diffusion models are secretly time-agnostic masked models and exploit inaccurate categorical sampling. *arXiv preprint arXiv:2409.02908*, 2024.
- Zheng, L., Yuan, J., Yu, L., and Kong, L. A reparameterized discrete diffusion model for text generation. *ArXiv*, abs/2302.05737, 2023.

Appendix

A. Auxiliary Lemma

In this section, we present some technical lemmas for the proof of our main results.

Lemma A.1 (Upper Bound for Multi-tokens Sampling). *Let $\mathbf{X} = (X_1, X_2, \dots, X_k) \in [N]^k$ be a random vector following the distribution q , where each component X_i follows the marginal distribution q_i . Define $\tilde{\mathbf{X}} = (\tilde{X}_1, \tilde{X}_2, \dots, \tilde{X}_k) \sim p$ as another random vector, where the components \tilde{X}_i are sampled independently according to p_i . Let $\delta = \max_i \{D_{\text{KL}}(q_i \| p_i)\}$, then, the KL divergence between p and q satisfies the inequality:*

$$D_{\text{KL}}(q \| p) \leq (k - 1) \log N + k\delta.$$

Proof. Using the chain rule for probabilities, the KL divergence can be written as:

$$D_{\text{KL}}(q \| p) = \mathbb{E}_q \left[\sum_{i=1}^k \log \left(\frac{q_i(x_i | \mathbf{x}_{<i})}{p_i(x_i)} \right) \right],$$

where $\mathbf{x}_{<i} = (x_1, \dots, x_{i-1})$. For $i = 1$, there are no preceding variables, so:

$$\mathbb{E}_q \left[\log \left(\frac{q_1(x_1)}{p_1(x_1)} \right) \right] = D_{\text{KL}}(q_1 \| p_1).$$

For $i > 1$, we bound:

$$\mathbb{E}_q \left[\log \left(\frac{q_i(x_i | \mathbf{x}_{<i})}{p_i(x_i)} \right) \right] \leq \mathbb{E}_q \left[\log \left(\frac{1}{p_i(x_i)} \right) \right].$$

Decomposing $\mathbb{E}_q [\log(1/p_i(x_i))]$, we get:

$$\mathbb{E}_q \left[\log \left(\frac{1}{p_i(x_i)} \right) \right] = \mathbb{E}_q \left[\log \left(\frac{q_i(x_i)}{p_i(x_i)} \right) \right] + \mathbb{E}_q \left[\log \left(\frac{1}{q_i(x_i)} \right) \right].$$

The first term is $D_{\text{KL}}(q_i \| p_i)$, and the second term is $-\mathbb{E}_q [\log q_i(x_i)]$, which represents the entropy of q_i . Since the entropy of any distribution over $[N]$ is at most $\log N$, we have:

$$-\mathbb{E}_q [\log q_i(x_i)] \leq \log N.$$

Thus:

$$\mathbb{E}_q \left[\log \left(\frac{q_i(x_i | \mathbf{x}_{<i})}{p_i(x_i)} \right) \right] \leq D_{\text{KL}}(q_i \| p_i) + \log N.$$

Summing over all $i = 1, \dots, k$, we obtain:

$$D_{\text{KL}}(q \| p) = \sum_{i=1}^k \mathbb{E}_q \left[\log \left(\frac{q_i(x_i | \mathbf{x}_{<i})}{p_i(x_i)} \right) \right] \leq D_{\text{KL}}(q_1 \| p_1) + \sum_{i=2}^k (D_{\text{KL}}(q_i \| p_i) + \log N).$$

Reorganizing, we have:

$$D_{\text{KL}}(q \| p) \leq \sum_{i=1}^k D_{\text{KL}}(q_i \| p_i) + (k - 1) \log N.$$

Since $D_{\text{KL}}(q_i \| p_i) \leq \delta$ for all i , the total sum of marginal KL divergences is bounded by $k\delta$. Therefore:

$$D_{\text{KL}}(q \| p) \leq k\delta + (k - 1) \log N.$$

This completes the proof. □

Lemma A.2 (Chernoff Bound). *Let X_1, \dots, X_n be independent random variables taking values in $\{0, 1\}$. Define $X = \sum_{i=1}^n X_i$ as the sum of these independent random variables, and let $\mu = \mathbb{E}[X]$ denote the expected value of X . Then, the following probabilistic bounds hold:*

$$\begin{aligned} \Pr(X \geq (1 + \delta)\mu) &\leq e^{-\frac{\delta^2 \mu}{2 + \delta}}, & \text{for } \delta \geq 0, \\ \Pr(X \leq (1 - \delta)\mu) &\leq e^{-\frac{\delta^2 \mu}{2}}, & \text{for } 0 < \delta < 1. \end{aligned}$$

Lemma A.3 (Pinsker’s Inequality). *Let p and q be two probability distributions. Then, the total variation distance between these distributions satisfies:*

$$D_{\text{TV}}(p, q) \leq \sqrt{\frac{1}{2} D_{\text{KL}}(p \| q)}.$$

Specifically, since $D_{\text{TV}}(p, q) = \frac{1}{2} \|p - q\|_1$, the following inequality holds:

$$\|p - q\|_1 \leq \sqrt{2 D_{\text{KL}}(p \| q)}.$$

B. Proof for Theorem 4.2

This section provides the complete proof of Theorem 4.2. We first outline the proof strategy, then present the detailed arguments with supporting lemmas and definitions.

Our proof rests on reformulating TER bounds through KL divergence and carefully analyzing dependencies in the n-gram setting. The key steps are:

- We establish a connection between the perplexity of the discrete diffusion model and the KL divergence between generated and data distributions. This involves deriving an upper bound on KL divergence using expected divergence over reverse processes (Lemma B.2) and decomposing this divergence into per-step conditional KL terms (Lemma B.3).
- We analyze n-gram model dependencies through a rigorous characterization of reverse processes (Definition B.1) and separators— $(n - 1)$ continuous sampled tokens that create independent intervals (Definition B.4). This leads to a precise formulation of per-step dependencies using these separators (Definition B.5).
- We derive an upper bound for the KL divergence between generated and data distributions based on the number of per-step dependencies (Lemmas B.8 and B.9).
- We employ probabilistic bounds to analyze and bound the number of per-step dependencies (Lemmas A.1, B.10 and B.11).
- Finally, we demonstrate the existence of a schedule achieving small KL divergence with $O(\frac{n-1}{\epsilon^n})$ steps by constructing an efficient sampling schedule using the preceding lemmas (Lemma B.12).

To begin the formal proof, we introduce key definitions for analyzing the discrete diffusion process. Consider a masking schedule α_t and a sequence of sampling time steps $t_i = \frac{N-i}{N}$. For a sequence of length L , we define an instance of the discretization of the reverse process τ as follows:

Definition B.1 (An Instance of Reverse Process). Let $\tau = (\mathcal{M}_1, \mathcal{M}_2, \dots, \mathcal{M}_N)$ represent a reverse process, where $\mathcal{M}_i = \{l_{ij}\}$ denotes the set of locations sampled at step i . For a sequence of length L , the sets \mathcal{M}_i satisfy the following conditions:

$$\bigcup_{i \in [N]} \mathcal{M}_i = [L] \quad \text{and} \quad \bigcap_{i \in [N]} \mathcal{M}_i = \emptyset.$$

Specifically, we denote $\mathcal{M}_{<i}$ as the union of all locations sampled prior to step t_i :

$$\mathcal{M}_{<i} = \bigcup_{j < i} \mathcal{M}_j.$$

Under a given instance of the reverse process τ , at each time step $t_i = \frac{N-i}{N}$, the set of locations $\mathcal{M}_i = \{l_{ij}\}$ is sampled. Let \tilde{x}_i denote the tokens associated with the locations sampled at time step t_i . Given the masking schedule α_t , there exist multiple possible instances of the reverse process. We denote the distribution over these instances by $\text{REVR}(\alpha_t, N, L)$.

Lemma B.2 (KL Divergence Upper Bound for the Masking Schedule). *Let q denote the data distribution over sequences of length L , and let p denote the distribution over sequences of length L generated by the reverse model p_θ with masking schedule α_t and N sampling steps. The KL divergence between q and p satisfies the following upper bound:*

$$D_{\text{KL}}(q\|p) \leq \mathbb{E}_{\tau \sim \text{REVR}(\alpha_t, N, L)} D_{\text{KL}}(q\|p(\cdot|\tau)),$$

where the expectation is taken over the distribution of reverse processes τ induced by $\text{REVR}(\alpha_t, N, L)$.

Proof. Let \mathcal{X} denote the set of all possible generated sequences. Then, the KL divergence between q and p is given by:

$$D_{\text{KL}}(q\|p) = \sum_{\mathbf{x} \in \mathcal{X}} q(\mathbf{x}) \log \frac{q(\mathbf{x})}{p(\mathbf{x})}.$$

Let h denote the distribution over reverse processes $\tau \sim \text{REVR}(\alpha_t, N, L)$. Due to the convexity of $\log \frac{1}{x}$, by applying Jensen's inequality, we can obtain:

$$\log \frac{1}{p(\mathbf{x})} = \log \frac{1}{\sum_{\tau} h(\tau) \cdot p(\mathbf{x}|\tau)} \leq \sum_{\tau} h(\tau) \cdot \log \frac{1}{p(\mathbf{x}|\tau)}.$$

Since data distribution q is independent of reverse process τ :

$$q(\mathbf{x}) = q(\mathbf{x}|\tau), \quad \forall \tau.$$

Therefore, we have:

$$\log \frac{q(\mathbf{x})}{p(\mathbf{x})} \leq \sum_{\tau} h(\tau) \log \frac{q(\mathbf{x}|\tau)}{p(\mathbf{x}|\tau)}.$$

Substituting this back, we can get the final result:

$$\begin{aligned} D_{\text{KL}}(q\|p) &\leq \sum_{\mathbf{x} \in \mathcal{X}} \sum_{\tau} h(\tau) q(\mathbf{x}) \log \frac{q(\mathbf{x}|\tau)}{p(\mathbf{x}|\tau)} \\ &= \sum_{\tau} h(\tau) \sum_{\mathbf{x} \in \mathcal{X}} q(\mathbf{x}|\tau) \log \frac{q(\mathbf{x}|\tau)}{p(\mathbf{x}|\tau)} \\ &= \mathbb{E}_{\tau \sim \text{REVR}(\alpha_t, N, L)} D_{\text{KL}}(q(\cdot|\tau)\|p(\cdot|\tau)) \\ &= \mathbb{E}_{\tau \sim \text{REVR}(\alpha_t, N, L)} D_{\text{KL}}(q\|p(\cdot|\tau)). \end{aligned}$$

□

We next establish an upper bound for the KL divergence between the distribution of sequences sampled under an instance of the reverse process τ and the ground-truth distribution in the n -gram setting. To achieve this, we leverage the chain rule for KL divergence, which allows decomposition of the KL divergence of the entire sequence into a summation of the KL divergences at each individual step of the process.

Lemma B.3 (KL Divergence Decomposition for the Reverse Process). *Consider an instance of reverse process $\tau = (\mathcal{M}_1, \mathcal{M}_2, \dots, \mathcal{M}_N) \sim \text{REVR}(\alpha_t, N, L)$. Let $\tilde{\mathbf{x}}_i$ denote the set of tokens corresponding to the locations sampled at time step t_i , and $\tilde{\mathbf{x}}_{<i}$ denote the set of tokens sampled at all steps prior to step t_i . The KL divergence between the ground-truth distribution q and the distribution p_τ generated by the reverse process τ and reverse model p_θ satisfies the following decomposition:*

$$D_{\text{KL}}(q\|p_\tau) = \sum_{i=1}^N \mathbb{E}_{\tilde{\mathbf{x}}_{<i}} D_{\text{KL}}(q(\tilde{\mathbf{x}}_i|\tilde{\mathbf{x}}_{<i})\|p_\tau(\tilde{\mathbf{x}}_i|\tilde{\mathbf{x}}_{<i})),$$

Proof. Given the reverse process τ , the reverse model samples $\tilde{\mathbf{x}}_i$ sequentially from $i = 1$ to N , and the probability of sampling $\tilde{\mathbf{x}}_i$ at step t_i depends only on the previously sampled tokens $\tilde{\mathbf{x}}_{<i}$. Therefore, the distribution $p(\mathbf{x})$ can be factorized as:

$$p_\tau(\mathbf{x}) = \prod_{i=1}^N p_\tau(\tilde{\mathbf{x}}_i|\tilde{\mathbf{x}}_{<i}).$$

On the other hand, since the data distribution q is independent of the reverse process τ , it can similarly be decomposed as:

$$q(\mathbf{x}) = \prod_{i=1}^N q(\tilde{\mathbf{x}}_i | \tilde{\mathbf{x}}_{<i}).$$

Applying the chain rule for KL divergence, we obtain:

$$D_{\text{KL}}(q \| p_\tau) = \sum_{i=1}^N \mathbb{E}_{\tilde{\mathbf{x}}_{<i}} D_{\text{KL}}(q(\tilde{\mathbf{x}}_i | \tilde{\mathbf{x}}_{<i}) \| p_\tau(\tilde{\mathbf{x}}_i | \tilde{\mathbf{x}}_{<i})).$$

□

Next, we derive an upper bound for the KL divergence at each step of the reverse process. In the n -gram setting, it is important to note that, at step t_i , the tokens $x_{l_{ij}}$ and $x_{l_{ij}'}$ are conditionally independent if there are at least $n - 1$ consecutive tokens between the positions l_{ij} and l_{ij}' that have already been sampled prior to step i . Under this condition, sampling these two tokens simultaneously incurs no sampling error, as the distributions of $x_{l_{ij}}$ and $x_{l_{ij}'}$ are independent.

To formalize this concept, we introduce a measure of dependencies among the tokens sampled in \mathcal{M}_i during the reverse process. For the i -th reverse step in the n -gram setting, the number of dependencies, denoted as $\text{DEP}_n(\mathcal{M}_i, \mathcal{M}_{<i})$, is determined by the structure of $\mathcal{M}_{<i}$. Specifically, it depends on the number of separators in $\mathcal{M}_{<i}$, denoted as $\text{SEP}_n(\mathcal{M}_{<i})$, as described in the following definition.

Definition B.4 (Number of Separators in a Reverse Step). Consider a reverse process $\tau = (\mathcal{M}_1, \mathcal{M}_2, \dots, \mathcal{M}_N)$, where $\mathcal{M}_{<i} = \bigcup_{j < i} \mathcal{M}_j$ represents the union of all previously sampled location sets. The set $\mathcal{M}_{<i}$ can be partitioned into several contiguous segments. Let $\mathcal{S}_1, \mathcal{S}_2, \dots, \mathcal{S}_k$ denote the segments containing at least $n - 1$ consecutive tokens (i.e., $|\mathcal{S}_j| \geq n - 1$) with the maximum k . We refer to these segments as separators, and denote the number of separators in the set $\mathcal{M}_{<i}$ as:

$$\begin{aligned} \text{SEP}_n(\mathcal{M}_{<i}) &= \max k \\ \text{s.t. } & |\mathcal{S}_j| \geq n - 1, \mathcal{S}_j \subset \mathcal{M}_{<i}, \quad \forall j \in [k], \\ & \mathcal{S}_j \cap \mathcal{S}_{j'} = \emptyset, \quad \forall j \neq j'. \end{aligned}$$

Note that if a contiguous segment \mathcal{S} in $\mathcal{M}_{<i}$ contains at least $d(n - 1)$ consecutive tokens, where d is an integer, then \mathcal{S} consists of at least d separators.

Definition B.5 (Number of Dependencies in a Reverse Step). Consider a reverse process $\tau = (\mathcal{M}_1, \mathcal{M}_2, \dots, \mathcal{M}_N)$. The separators of $\mathcal{M}_{<i}$ divide the sequence into at most $\text{SEP}_n(\mathcal{M}_{<i}) + 1$ disjoint intervals $\mathcal{I}_1, \mathcal{I}_2, \dots, \mathcal{I}_k$. Under the n -gram setting, the sampling within each interval is independent of the sampling in other intervals. The number of dependencies of step t_i is defined as the number of intervals \mathcal{I}_p (for $p = 1, \dots, k$) that contain at least one location in \mathcal{M}_i :

$$\text{DEP}_n(\mathcal{M}_i, \mathcal{M}_{<i}) = |\mathcal{M}_i| - \sum_{p=1}^k \mathbb{I}[\mathcal{I}_p \cap \mathcal{M}_i \neq \emptyset],$$

where \mathbb{I} is the indicator function.

To illustrate this definition, we provide the following example:

Example B.6 (Computing Dependencies in the n -gram Setting). Consider a token sequence of length 10, denoted as $\mathbf{x} = (x_1, x_2, \dots, x_{10})$, with $n = 4$. Let the previously sampled location set be $\mathcal{M}_{<i} = \{2, 3, 4, 6, 7\}$ and the current location set be $\mathcal{M}_i = \{1, 5, 9\}$.

1. **Identify contiguous segments in $\mathcal{M}_{<i}$ containing at least $n - 1 = 3$ consecutive tokens:** The set $\mathcal{M}_{<i} = \{2, 3, 4, 6, 7\}$ forms the following contiguous segments:

$$\{2, 3, 4\} \quad \text{and} \quad \{6, 7\}.$$

Only the segment $\{2, 3, 4\}$ contains at least $n - 1 = 3$ consecutive tokens. Thus, we have $\mathcal{S}_1 = \{2, 3, 4\}$. The sequence is then divided into the following disjoint intervals:

$$\mathcal{I}_1 = \{1\}, \quad \mathcal{I}_2 = \{5, 6, 7, 8, 9, 10\}.$$

2. **Determine which intervals overlap with $\mathcal{M}_i = \{1, 5, 9\}$:** Token 1 belongs to interval \mathcal{I}_1 , and tokens 5 and 9 belong to interval \mathcal{I}_2 .
3. **Compute the number of dependencies:** The number of dependencies is:

$$\text{DEP}_n(\mathcal{M}_i, \mathcal{M}_{<i}) = |\mathcal{M}_i| - \sum_{p=1}^k \mathbb{I}[\mathcal{I}_p \cap \mathcal{M}_i \neq \emptyset] = 3 - 2 = 1.$$

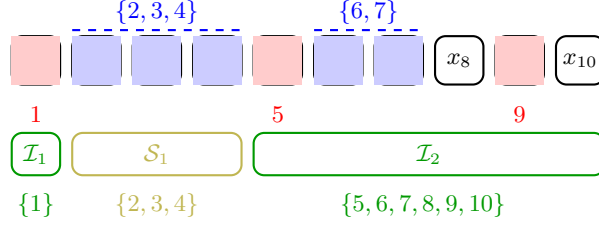


Figure 3. Illustration of the example for computing dependencies in the n -gram setting. Tokens x_2, x_3, x_4, x_6, x_7 (blue) represent the previously sampled location set $\mathcal{M}_{<i}$, forming two contiguous segments: $\{2, 3, 4\}$ and $\{6, 7\}$. The current sampled locations x_1, x_5, x_9 (red) overlap with disjoint intervals $\mathcal{I}_1 = \{1\}$ and $\mathcal{I}_2 = \{5, 6, 7, 8, 9, 10\}$. The number of dependencies is computed as $\text{DEP}_n(\mathcal{M}_i, \mathcal{M}_{<i}) = |\mathcal{M}_i| - (\text{number of overlapping intervals}) = 3 - 2 = 1$.

This example demonstrates how dependencies are computed, highlighting the interaction between previously sampled locations and the current reverse step. Such formalization is critical for understanding the efficiency and accuracy of discrete diffusion processes.

Finally, we extend this concept to define the total number of dependencies across an entire reverse process:

Definition B.7 (Number of Dependencies in a Reverse Process). Consider a reverse process $\tau = (\mathcal{M}_1, \mathcal{M}_2, \dots, \mathcal{M}_N)$. Under the n -gram setting, the total number of dependencies in the process is defined as the sum of the dependencies across all steps:

$$\text{DEP}_n(\tau) = \sum_{i=1}^N \text{DEP}_n(\mathcal{M}_i, \mathcal{M}_{<i}).$$

Using the definition of $\text{DEP}_n(\tau)$, we can bound the KL divergence between the distribution of sequences sampled under an instance of the reverse process and the ground-truth distribution in the n -gram setting.

Lemma B.8 (KL Divergence Upper Bound for the Instance of Reverse Process). Let q denote the data distribution for sequences of length L , and let p denote the distribution of sequences of length L generated by reverse model p_θ via the reverse process τ . Under Assumption 4.1, the following upper bound holds:

$$D_{\text{KL}}(q \| p(\cdot | \tau)) \leq \text{DEP}_n(\tau) \log |\mathcal{V}| + L \epsilon_{\text{learning}},$$

where \mathcal{V} denote the vocabulary.

Proof. Using Lemma B.3, we have:

$$D_{\text{KL}}(q \| p_\tau) = \sum_{i=1}^N \mathbb{E}_{\tilde{\mathbf{x}}_{<i}} D_{\text{KL}}(q(\tilde{\mathbf{x}}_i | \tilde{\mathbf{x}}_{<i}) \| p_\tau(\tilde{\mathbf{x}}_i | \tilde{\mathbf{x}}_{<i})).$$

For each time step t_i :

$$\mathbb{E}_{\tilde{\mathbf{x}}_{<i}} D_{\text{KL}}(q(\tilde{\mathbf{x}}_i | \tilde{\mathbf{x}}_{<i}) \| p_\tau(\tilde{\mathbf{x}}_i | \tilde{\mathbf{x}}_{<i})) = \mathbb{E}_{\tilde{\mathbf{x}}_{<i}} \sum_{\tilde{\mathbf{x}}_i \in \mathcal{V}^{|\mathcal{M}_i|}} q(\tilde{\mathbf{x}}_i | \tilde{\mathbf{x}}_{<i}) \log \frac{q(\tilde{\mathbf{x}}_i | \tilde{\mathbf{x}}_{<i})}{p_\tau(\tilde{\mathbf{x}}_i | \tilde{\mathbf{x}}_{<i})}.$$

Given \mathcal{M}_i and $\mathcal{M}_{<i}$, the tokens $\tilde{\mathbf{x}}_i$ at step t_i can be partitioned into independently sampled token sets $\tilde{\mathbf{x}}_i^{(1)}, \dots, \tilde{\mathbf{x}}_i^{(m)}$ with k_j denoting the size of each token set:

$$k_j = |\tilde{\mathbf{x}}_i^{(j)}|, \quad j \in [m], \quad m = |\mathcal{M}_i| - \text{DEP}_n(\mathcal{M}_i, \mathcal{M}_{<i}).$$

Using the independence, for each $\tilde{\mathbf{x}}_{<i}$, we can decompose the sum into:

$$\begin{aligned} \sum_{\tilde{\mathbf{x}}_i \in \mathcal{V}^{|\mathcal{M}_i|}} q(\tilde{\mathbf{x}}_i | \tilde{\mathbf{x}}_{<i}) \log \frac{q(\tilde{\mathbf{x}}_i | \tilde{\mathbf{x}}_{<i})}{p_\tau(\tilde{\mathbf{x}}_i | \tilde{\mathbf{x}}_{<i})} &= \sum_{j=1}^m \sum_{\tilde{\mathbf{x}}_i^{(j)} \in \mathcal{V}^{k_j}} q(\tilde{\mathbf{x}}_i^{(j)} | \tilde{\mathbf{x}}_{<i}) \log \frac{q(\tilde{\mathbf{x}}_i^{(j)} | \tilde{\mathbf{x}}_{<i})}{p_\tau(\tilde{\mathbf{x}}_i^{(j)} | \tilde{\mathbf{x}}_{<i})} \\ &= \sum_{j=1}^m D_{\text{KL}}(q(\tilde{\mathbf{x}}_i^{(j)} | \tilde{\mathbf{x}}_{<i}) \| p_\tau(\tilde{\mathbf{x}}_i^{(j)} | \tilde{\mathbf{x}}_{<i})). \end{aligned}$$

Under Assumption 4.1, the KL divergence between q and p_θ is bounded by:

$$D_{\text{KL}}(q_{0|t}(x_0^i | \mathbf{x}_t) \| p_\theta(x_0^i | \mathbf{x}_t)) < \epsilon_{\text{learning}}, \quad \forall t \text{ and } \mathbf{x}_t.$$

By Lemma A.1, we know that:

$$D_{\text{KL}}(q(\tilde{\mathbf{x}}_i^{(j)} | \tilde{\mathbf{x}}_{<i}) \| p_\tau(\tilde{\mathbf{x}}_i^{(j)} | \tilde{\mathbf{x}}_{<i})) \leq (k_j - 1) \log |\mathcal{V}| + k_j \epsilon_{\text{learning}}.$$

Substituting back:

$$\sum_{\tilde{\mathbf{x}}_i \in \mathcal{V}^{|\mathcal{M}_i|}} q(\tilde{\mathbf{x}}_i | \tilde{\mathbf{x}}_{<i}) \log \frac{q(\tilde{\mathbf{x}}_i | \tilde{\mathbf{x}}_{<i})}{p_\tau(\tilde{\mathbf{x}}_i | \tilde{\mathbf{x}}_{<i})} \leq \sum_{j=1}^m (k_j - 1) \log |\mathcal{V}| + k_j \epsilon_{\text{learning}}.$$

Using the fact that

$$\sum_{j=1}^m (k_j - 1) = |\mathcal{M}_i| - m = \text{DEP}_n(\mathcal{M}_i, \mathcal{M}_{<i}), \quad \sum_{j=1}^m k_j = |\mathcal{M}_i|$$

we can obtain:

$$\mathbb{E}_{\tilde{\mathbf{x}}_{<i}} D_{\text{KL}}(q(\tilde{\mathbf{x}}_i | \tilde{\mathbf{x}}_{<i}) \| p_\tau(\tilde{\mathbf{x}}_i | \tilde{\mathbf{x}}_{<i})) \leq \text{DEP}_n(\mathcal{M}_i, \mathcal{M}_{<i}) \log |\mathcal{V}| + |\mathcal{M}_i| \epsilon_{\text{learning}}.$$

Thus, combined with the definition of $\text{DEP}_n(\tau)$ and $p_\tau = p(\cdot | \tau)$, we can draw the final conclusion:

$$\begin{aligned} D_{\text{KL}}(q \| p(\cdot | \tau)) &\leq \sum_{i=1}^N (\text{DEP}_n(\mathcal{M}_i, \mathcal{M}_{<i}) \log |\mathcal{V}| + |\mathcal{M}_i| \epsilon_{\text{learning}}) \\ &= \text{DEP}_n(\tau) \log |\mathcal{V}| + L \epsilon_{\text{learning}}. \end{aligned}$$

□

The above Lemma directly leads to the bound for the KL divergence between the distribution of sequences generated by the reverse model with a given masking schedule and the ground-truth distribution in the n -gram setting.

Lemma B.9 (KL Divergence Upper Bound for a Masking Schedule). *Let q denote the data distribution over sequences of length L , and let p denote the distribution over sequences of length L generated by the reverse model p_θ with masking schedule α_t and N reverse steps. Under Assumption 4.1, the KL divergence between q and p satisfies the following upper bound:*

$$D_{\text{KL}}(q \| p) \leq \log |\mathcal{V}| \sum_{i=1}^N \mathbb{E}_{\tau \sim \text{REVR}(L, \alpha_t, N)} \text{DEP}_n(\mathcal{M}_i, \mathcal{M}_{<i}) + L \epsilon_{\text{learning}}.$$

Proof. By Lemma B.2, we can obtain:

$$D_{\text{KL}}(q \| p) \leq \mathbb{E}_{\tau \sim \text{REVR}(\alpha_t, N, L)} D_{\text{KL}}(q \| p(\cdot | \tau)).$$

Applying Lemma B.8 to the instances of reverse process, we can conclude that:

$$\begin{aligned} D_{\text{KL}}(q||p) &\leq \mathbb{E}_{\tau \sim \text{REVR}(\alpha_t, N, L)} \sum_{i=1}^N \text{DEP}_n(\mathcal{M}_i, \mathcal{M}_{<i}) \log |\mathcal{V}| + L\epsilon_{\text{learning}} \\ &= \log |\mathcal{V}| \sum_{i=1}^N \mathbb{E}_{\tau \sim \text{REVR}(L, \alpha_t, N)} \text{DEP}_n(\mathcal{M}_i, \mathcal{M}_{<i}) + L\epsilon_{\text{learning}}. \end{aligned}$$

□

For the final estimation, we need to derive an upper bound for the expected number of dependencies at each reverse step. First, we use Chernoff Bound to control the number of separators and new locations at each reverse step for a given masking schedule.

Lemma B.10 (Bounds on Separator and New Location Count at Each Reverse Step). *Given a sequence of length L , a masking schedule α_t , and N reverse steps. Assume that L is divisible by $n - 1$. Given the time step $t_i = \frac{N-i}{N}$, let NEW denote the number of locations sampled at step t_i , and SEP_n denote the number of separators in the previously sampled locations. Under the n -gram setting, the following bounds hold for NEW and SEP_n :*

$$\begin{aligned} \Pr\left(\text{SEP}_n \leq \frac{Lp_i^{n-1}}{2(n-1)}\right) &\leq e^{-\frac{Lp_i^{n-1}}{8(n-1)}}, \\ \Pr(\text{NEW} \geq 2L\delta_i) &\leq e^{-\frac{L\delta_i}{3}}, \end{aligned}$$

where $p_i = \alpha_{t_{i-1}}$ and $\delta_i = \alpha_{t_i} - \alpha_{t_{i-1}}$.

Proof. Given a masking schedule α_t , using the expression of true reverse process in Equation (2) and $\alpha_1 = 0$, we can compute the probability $p^{(i)}$ of a token being sampled at time step t_i to be:

$$p^{(i)} = \frac{\alpha_{t_i} - \alpha_{t_{i-1}}}{1 - \alpha_{t_{i-1}}} \cdot \prod_{j=1}^{i-1} \frac{1 - \alpha_{t_j}}{1 - \alpha_{t_{j-1}}} = \alpha_{t_i} - \alpha_{t_{i-1}} = \delta_i.$$

Therefore, δ_i is the probability of a location being sampled at time step t_i . Summing up δ_i , we can know that $p_i = \sum_{j=1}^{i-1} \delta_j$ is the probability of a location being sampled prior to time step t_i .

To derive a bound for SEP_n , we partition the sequence into $\frac{L}{n-1}$ intervals, each of length $n - 1$. For a given interval, the probability that all locations within the interval have been sampled prior to step t_i is p_i^{n-1} . Define $X_j = 1$ if the locations in the j -th interval have been sampled prior to t_i , and $X_j = 0$ otherwise. The random variables $X_1, X_2, \dots, X_{\frac{L}{n-1}}$ are independent and satisfy the following expectation:

$$\mathbb{E}_{\tau \sim \text{REVR}(L, \alpha_t, N)} \sum_{j=1}^{\frac{L}{n-1}} X_j = \frac{Lp_i^{n-1}}{n-1}.$$

By the definition of SEP_n , we know that:

$$\text{SEP}_n \geq \sum_{j=1}^{\frac{L}{n-1}} X_j.$$

Applying Lemma A.2 to the sum of X_j , we derive:

$$\Pr\left(\text{SEP}_n \leq \frac{Lp_i^{n-1}}{2(n-1)}\right) \leq \Pr\left(\sum_{j=1}^{\frac{L}{n-1}} X_j \leq \frac{Lp_i^{n-1}}{2(n-1)}\right) \leq e^{-\frac{Lp_i^{n-1}}{8(n-1)}}.$$

Next, we consider the bound for NEW . Given that the sequence contains L locations and the probability of sampling any specific location at step t_i is δ_i , the expected number of new locations sampled at t_i is given by:

$$\mathbb{E}_{\tau \sim \text{REVR}(L, \alpha_t, N)} \text{NEW} = L\delta_i.$$

Since the sampling of each location occurs independently, applying Lemma A.2, we have:

$$\Pr(\text{NEW} \geq 2L\delta_i) \leq e^{-\frac{L\delta_i}{3}}.$$

□

Using the above lemma, we can divide the estimation for the number of dependencies into three cases, and derive the bound case by case. This is achieved by using a variety of means and careful estimations.

Lemma B.11 (Upper Bound for the Expectation of Dependencies at Each Reverse Step). *Given a sequence of length L , a masking schedule α_t , and N reverse steps. Assume $L\delta_i > 1$, then the expected number of dependencies at time step $t_i = \frac{N-i}{N}$ satisfies:*

$$\mathbb{E}_{\tau \sim \text{REVR}(L, \alpha_t, N)} \text{DEP}_n(\mathcal{M}_i, \mathcal{M}_{<i}) \leq \frac{9}{3 + L\delta_i} + \frac{C(n-1)L\delta_i^2}{p_i^{n-1}},$$

where $p_i = \alpha_{t_{i-1}}$, $\delta_i = \alpha_{t_i} - \alpha_{t_{i-1}}$, and C is a constant.

Proof. By Lemma B.10, at step t_i , the following bounds hold:

$$\Pr\left(\text{SEP}_n \leq \frac{Lp_i^{n-1}}{2(n-1)}\right) \leq e^{-\frac{Lp_i^{n-1}}{8(n-1)}},$$

$$\Pr(\text{NEW} \geq 2L\delta_i) \leq e^{-\frac{L\delta_i}{3}}.$$

Since $\text{DEP}_n(\mathcal{M}_i, \mathcal{M}_{<i}) \geq 0$, its expectation can be decomposed into three components:

$$\begin{aligned} \mathbb{E}_{\tau \sim \text{REVR}(L, \alpha_t, N)} \text{DEP}_n(\mathcal{M}_i, \mathcal{M}_{<i}) &= \Pr(\text{NEW} \geq 2L\delta_i) \cdot \mathbb{E}_{\tau \sim \text{REVR}(L, \alpha_t, N)} \text{DEP}_n(\mathcal{M}_i, \mathcal{M}_{<i}) \quad \text{(Case 1)} \\ &\quad + \Pr\left(\text{SEP}_n \leq \frac{Lp_i^{n-1}}{2(n-1)}, \text{NEW} < 2L\delta_i\right) \cdot \\ &\quad \mathbb{E}_{\tau \sim \text{REVR}(L, \alpha_t, N)} \text{DEP}_n(\mathcal{M}_i, \mathcal{M}_{<i}) \quad \text{(Case 2)} \\ &\quad + \Pr\left(\text{SEP}_n > \frac{Lp_i^{n-1}}{2(n-1)}, \text{NEW} < 2L\delta_i\right) \cdot \\ &\quad \mathbb{E}_{\tau \sim \text{REVR}(L, \alpha_t, N)} \text{DEP}_n(\mathcal{M}_i, \mathcal{M}_{<i}) \quad \text{(Case 3)} \end{aligned}$$

We estimate these three cases separately.

Case 1: $\text{NEW} \geq 2L\delta_i$.

By the definitions of $\text{DEP}_n(\mathcal{M}_i, \mathcal{M}_{<i})$ and NEW , we have:

$$\text{DEP}_n(\mathcal{M}_i, \mathcal{M}_{<i}) \leq |\mathcal{M}_i| = \text{NEW}.$$

Substituting this into the estimation, we obtain:

$$\Pr(\text{NEW} \geq 2L\delta_i) \cdot \mathbb{E}_{\tau \sim \text{REVR}(L, \alpha_t, N)} \text{DEP}_n(\mathcal{M}_i, \mathcal{M}_{<i}) \leq \Pr(\text{NEW} \geq 2L\delta_i) \cdot \mathbb{E}_{\tau \sim \text{REVR}(L, \alpha_t, N)} \text{NEW}_{\text{NEW} \geq 2L\delta_i}$$

Since $\text{DEP}_n(\mathcal{M}_i, \mathcal{M}_{<i}) \geq 0$, the expectation can be expressed as an integral of the tail probability:

$$\mathbb{E}_{\tau \sim \text{REVR}(L, \alpha_t, N)} \text{NEW}_{\text{NEW} \geq 2L\delta_i} = \int_{2L\delta_i}^{+\infty} \Pr(\text{NEW} \geq x \mid \text{NEW} \geq 2L\delta_i) dx.$$

It directly follows that:

$$\begin{aligned}
 \Pr(\text{NEW} \geq 2L\delta_i) \cdot \mathbb{E}_{\tau \sim \text{REVR}(L, \alpha_t, N)} \Pr(\text{NEW} \geq 2L\delta_i) &= \Pr(\text{NEW} \geq 2L\delta_i) \cdot \int_{2L\delta_i}^{+\infty} \Pr(\text{NEW} \geq x \mid \text{NEW} \geq 2L\delta_i) dx \\
 &= \int_{2L\delta_i}^{+\infty} \Pr(\text{NEW} \geq x \mid \text{NEW} \geq 2L\delta_i) \Pr(\text{NEW} \geq 2L\delta_i) dx \\
 &= \int_{2L\delta_i}^{+\infty} \Pr(\text{NEW} \geq x) dx.
 \end{aligned}$$

Using the same trick as Lemma B.10, applying Lemma A.2, we can derive the bound for probability $\Pr(\text{NEW} \geq x)$ as:

$$\Pr(\text{NEW} \geq x) \leq e^{-\frac{(x-L\delta_i)^2}{x+L\delta_i}}.$$

Note that $\text{NEW} \leq L$, we only need to consider $2\delta_i \leq 1$. In this case, we have:

$$\int_{2L\delta_i}^{+\infty} \Pr(\text{NEW} \geq x) dx \leq \int_{2L\delta_i}^L e^{-\frac{(x-L\delta_i)^2}{x+L\delta_i}} dx$$

Let $y = x - L\delta_i \in [L\delta_i, L(1 - \delta_i)]$, the integral can be rewritten as:

$$\int_{2L\delta_i}^{+\infty} \Pr(\text{NEW} \geq x) dx \leq \int_{L\delta_i}^{L(1-\delta_i)} e^{-\frac{y^2}{y+2L\delta_i}} dy.$$

Observe that $y + 2L\delta_i \leq 3y$, we can obtain:

$$\int_{2L\delta_i}^{+\infty} \Pr(\text{NEW} \geq x) dx \leq \int_{L\delta_i}^{L(1-\delta_i)} e^{-\frac{y^2}{3y}} dy = 3 \left(e^{-\frac{L\delta_i}{3}} - e^{-\frac{L(1-\delta_i)}{3}} \right) = 3e^{-\frac{L\delta_i}{3}} \left(1 - e^{-\frac{L(1-2\delta_i)}{3}} \right).$$

Using the fact that $e^{-x} \leq \frac{1}{1+x}$ for $x \geq 0$, we have the upper bound:

$$3e^{-\frac{L\delta_i}{3}} \left(1 - e^{-\frac{L(1-2\delta_i)}{3}} \right) \leq 3e^{-\frac{L\delta_i}{3}} \leq \frac{9}{3 + L\delta_i}.$$

Combining the above results, we know that:

$$\Pr(\text{NEW} \geq 2L\delta_i) \cdot \mathbb{E}_{\tau \sim \text{REVR}(L, \alpha_t, N)} \Pr(\text{NEW} \geq 2L\delta_i) \leq \frac{9}{3 + L\delta_i}.$$

Case 2: $\text{SEP}_n \leq \frac{Lp_i^{n-1}}{2(n-1)}$ and $\text{NEW} < 2L\delta_i$.

Similar to Case 1, we have:

$$\text{DEP}_n(\mathcal{M}_i, \mathcal{M}_{<i}) \leq \text{NEW} < 2L\delta_i,$$

so the expectation also follows:

$$\mathbb{E}_{\tau \sim \text{REVR}(L, \alpha_t, N)} \text{DEP}_n(\mathcal{M}_i, \mathcal{M}_{<i}) < 2L\delta_i.$$

$$\begin{aligned} \text{SEP}_n &\leq \frac{Lp_i^{n-1}}{2(n-1)} \\ \text{NEW} &< 2L\delta_i \end{aligned}$$

Using the probability bound, it follows that:

$$\Pr\left(\text{SEP}_n \leq \frac{Lp_i^{n-1}}{2(n-1)}, \text{NEW} < 2L\delta_i\right) \leq \Pr\left(\text{SEP}_n \leq \frac{Lp_i^{n-1}}{2(n-1)}\right) \leq e^{-\frac{Lp_i^{n-1}}{8(n-1)}}.$$

Since $e^{-x} \leq \frac{1}{1+x}$ for $x \geq 0$:

$$e^{-\frac{Lp_i^{n-1}}{8(n-1)}} \leq \frac{8(n-1)}{Lp_i^{n-1} + 8(n-1)}.$$

Combining these results, we obtain:

$$\Pr\left(\text{SEP}_n \leq \frac{Lp_i^{n-1}}{2(n-1)}, \text{NEW} < 2L\delta_i\right) \cdot \mathbb{E}_{\tau \sim \text{REVR}(L, \alpha_t, N)} \text{DEP}_n(\mathcal{M}_i, \mathcal{M}_{<i}) \leq \frac{16(n-1)L\delta_i}{Lp_i^{n-1} + 8(n-1)}.$$

$\begin{matrix} \text{SEP}_n \leq \frac{Lp_i^{n-1}}{2(n-1)} \\ \text{NEW} < 2L\delta_i \end{matrix}$

Case 3: $\text{SEP}_n > \frac{Lp_i^{n-1}}{2(n-1)}$ and $\text{NEW} < 2L\delta_i$.

Apparently, we have:

$$\Pr\left(\text{SEP}_n > \frac{Lp_i^{n-1}}{2(n-1)}, \text{NEW} < 2L\delta_i\right) \leq 1.$$

Given a, b , let $\mathbb{E}_{a,b} \text{DEP}_n(\mathcal{M}_i, \mathcal{M}_{<i})$ denote the expectation of $\text{DEP}_n(\mathcal{M}_i, \mathcal{M}_{<i})$ under the condition of $\text{SEP}_n = a$ and $\text{NEW} = b$. In other words:

$$\mathbb{E}_{a,b} \text{DEP}_n(\mathcal{M}_i, \mathcal{M}_{<i}) = \mathbb{E}_{\tau \sim \text{REVR}(L, \alpha_t, N)} \text{DEP}_n(\mathcal{M}_i, \mathcal{M}_{<i})$$

$\begin{matrix} \text{SEP}_n = a \\ \text{NEW} = b \end{matrix}$

Since all the locations are sampled independently, and $\text{DEP}_n(\mathcal{M}_i, \mathcal{M}_{<i})$ depends only on the relative positions of separators in $\mathcal{M}_{<i}$ and the new locations in \mathcal{M}_i , the expectation $\mathbb{E}_{a,b} \text{DEP}_n(\mathcal{M}_i, \mathcal{M}_{<i})$ only depends on the ordering of separators and new locations.

Assume x_1, \dots, x_{a+b} are $a+b$ positions (not locations) in order. We can regard the process of ordering separators and new locations as the process of choosing b positions randomly from x_j . For $1 \leq j \leq a+b-1$, define $X_j = 1$ if x_j and x_{j+1} are both new locations, and $X_j = 0$ otherwise. By the definition of $\text{DEP}_n(\mathcal{M}_i, \mathcal{M}_{<i})$, we can obtain:

$$\text{DEP}_n(\mathcal{M}_i, \mathcal{M}_{<i}) = \sum_{j=1}^{a+b-1} X_j.$$

Since the b new locations are chosen randomly, the probability of $X_j = 1$ can be calculated as:

$$\Pr(X_j = 1) = \frac{C_{a+b-2}^{b-2}}{C_{a+b}^b} = \frac{b(b-1)}{(a+b)(a+b-1)}.$$

Therefore, the expectation of X_j is:

$$\mathbb{E}X_j = \frac{b(b-1)}{(a+b)(a+b-1)}.$$

Summing up, we have:

$$\mathbb{E}_{a,b} \text{DEP}_n(\mathcal{M}_i, \mathcal{M}_{<i}) = \mathbb{E} \sum_{j=1}^{a+b-1} X_j = (a+b-1)\mathbb{E}X_1 = \frac{b(b-1)}{a+b}.$$

Since $a > \frac{Lp_i^{n-1}}{2(n-1)}$ and $b < 2L\delta_i$, we can derive the upper bound for any a, b :

$$\frac{b(b-1)}{a+b} \leq \frac{b(b-1)}{\frac{Lp_i^{n-1}}{2(n-1)} + b} \leq \frac{2L\delta_i(2L\delta_i-1)}{\frac{Lp_i^{n-1}}{2(n-1)} + 2L\delta_i} \leq \frac{8(n-1)L\delta_i^2}{p_i^{n-1} + 4(n-1)\delta_i}.$$

Since this holds for all a and b , we can obtain:

$$\begin{aligned}
 & \Pr\left(\text{SEP}_n > \frac{Lp_i^{n-1}}{2(n-1)}, \text{NEW} < 2L\delta_i\right) \cdot \mathbb{E}_{\tau \sim \text{REVR}(L, \alpha_t, N)} \text{DEP}_n(\mathcal{M}_i, \mathcal{M}_{<i}) \\
 & \leq \mathbb{E}_{\tau \sim \text{REVR}(L, \alpha_t, N)} \text{DEP}_n(\mathcal{M}_i, \mathcal{M}_{<i}) \\
 & \quad \text{SEP}_n > \frac{Lp_i^{n-1}}{2(n-1)} \\
 & \quad \text{NEW} < 2L\delta_i \\
 & = \sum_{a > \frac{Lp_i^{n-1}}{2(n-1)}, b < 2L\delta_i} \Pr(\text{SEP}_n = a, \text{NEW} = b) \cdot \mathbb{E}_{a,b} \text{DEP}_n(\mathcal{M}_i, \mathcal{M}_{<i}) \\
 & \leq \frac{8(n-1)L\delta_i^2}{p_i^{n-1} + 4(n-1)\delta_i}.
 \end{aligned}$$

Summarize the above proof:

Combining the above three cases, we can obtain:

$$\mathbb{E}_{\tau \sim \text{REVR}(L, \alpha_t, N)} \text{DEP}_n(\mathcal{M}_i, \mathcal{M}_{<i}) \leq \frac{9}{3 + L\delta_i} + \frac{16(n-1)L\delta_i}{Lp_i^{n-1} + 8(n-1)} + \frac{8(n-1)L\delta_i^2}{p_i^{n-1} + 4(n-1)\delta_i}.$$

If we have the assumption $L\delta_i \geq 1$, it is easy to find that:

$$\begin{aligned}
 \mathbb{E}_{\tau \sim \text{REVR}(L, \alpha_t, N)} \text{DEP}_n(\mathcal{M}_i, \mathcal{M}_{<i}) & \leq \frac{9}{3 + L\delta_i} + \frac{16(n-1)\delta_i}{p_i^{n-1}} + \frac{8(n-1)L\delta_i^2}{p_i^{n-1}} \\
 & \leq \frac{9}{3 + L\delta_i} + \frac{16(n-1)L\delta_i^2}{p_i^{n-1}} + \frac{8(n-1)L\delta_i^2}{p_i^{n-1}} \\
 & \leq \frac{9}{3 + L\delta_i} + \frac{C(n-1)L\delta_i^2}{p_i^{n-1}}.
 \end{aligned}$$

Where $C = 24$ is a constant. □

Finally, we can derive the upper bound for the KL divergence between the distribution of sequences generated by the reverse model and the ground-truth distribution in the n -gram setting.

Lemma B.12 (Efficient Sampling with Small KL Divergence). *Let q denote the data distribution over sequences of length L , and let p denote the distribution over sequences of length L generated by the reverse model p_θ with a masking schedule α_t and N reverse steps. Assume that p_θ satisfies Assumption 4.1. For any $\epsilon > 0$, there exists a masking schedule α_t such that, for $L \geq \frac{3C(n-1)}{\epsilon^{n+\frac{1}{2}}}$, with $N = O\left(\frac{n-1}{\epsilon^n}\right)$ sampling steps, the KL divergence between q and p satisfies:*

$$\frac{D_{\text{KL}}(q||p)}{L \log |\mathcal{V}|} \leq 4\epsilon + \frac{\epsilon_{\text{learning}}}{\log |\mathcal{V}|}.$$

Proof. By Lemma B.9, we know that:

$$D_{\text{KL}}(q||p) \leq \log |\mathcal{V}| \sum_{i=1}^N \mathbb{E}_{\tau \sim \text{REVR}(L, \alpha_t, N)} \text{DEP}_n(\mathcal{M}_i, \mathcal{M}_{<i}) + L\epsilon_{\text{learning}}.$$

Note that at step t_1 , the reverse process can be bounded using Lemma A.1. By reviewing our proof process, it is easy to see that we can substitute $\text{DEP}_n(\mathcal{M}_1, \mathcal{M}_{<1})$ for $(|\mathcal{M}_1| - 1) \log |\mathcal{V}|$, where \mathcal{V} stands for the vocabulary. By the definition of δ_i , we know that:

$$\mathbb{E}_{\tau \sim \text{REVR}(L, \alpha_t, N)} (|\mathcal{M}_1| - 1) \log |\mathcal{V}| = (\delta_1 L - 1) \log |\mathcal{V}|.$$

Applying Lemma B.11 to $\text{DEP}_n(\mathcal{M}_i, \mathcal{M}_{<i})$, if $L\delta_i \geq 1$, we can obtain:

$$D_{\text{KL}}(q||p) \leq \delta_1 \log |\mathcal{V}| + \log |\mathcal{V}| \sum_{i=2}^N \left(\frac{9}{3 + L\delta_i} + \frac{C(n-1)L\delta_i^2}{p_i^{n-1}} \right) + L\epsilon_{\text{learning}}.$$

By the definition of p_i , we know that $p_2 = \delta_1$. For any small $\epsilon > 0$, consider the following masking schedule:

$$\delta_1 = \epsilon, \quad \delta_i = \delta = \frac{\epsilon^n}{C(n-1)}, \quad p_i = \delta_1 + (i-2)\delta, \quad \forall i \geq 2.$$

Then, for $L \geq \frac{1}{\delta}$, the KL divergence can be bounded by:

$$\begin{aligned} \frac{D_{\text{KL}}(q||p)}{L \log |\mathcal{V}|} &\leq \epsilon + \frac{9(N-1)}{L(3+L\delta)} + \sum_{i=2}^N \frac{C(n-1)\delta^2}{p_i^{n-1}} + \frac{\epsilon_{\text{learning}}}{\log |\mathcal{V}|} \\ &= \epsilon + \frac{9(1-\delta_1)}{L\delta(3+L\delta)} + \frac{C(n-1)\delta^2}{\delta_1^{n-1}} + \sum_{i=1}^{N-2} \frac{C(n-1)\delta^2}{(\delta_1 + i\delta)^{n-1}} + \frac{\epsilon_{\text{learning}}}{\log |\mathcal{V}|} \\ &\leq \epsilon + \frac{9}{L\delta(3+L\delta)} + \frac{C(n-1)\delta^2}{\delta_1^{n-1}} + \sum_{i=1}^{N-2} \frac{C(n-1)\delta^2}{(\delta_1 + i\delta)^n} + \frac{\epsilon_{\text{learning}}}{\log |\mathcal{V}|}. \end{aligned}$$

By simple calculations, we know that:

$$\frac{9}{L\delta(3+L\delta)} \leq \epsilon, \quad \text{if } L \geq \frac{3}{\delta\epsilon^{\frac{1}{2}}}.$$

It is clear that $\delta \leq 1$, so:

$$\frac{C(n-1)\delta^2}{\delta_1^{n-1}} \leq \epsilon\delta \leq \epsilon.$$

Since x^{-n} is convex on $[0, +\infty)$, the accumulation can be bounded by:

$$\begin{aligned} \sum_{i=1}^{N-2} \frac{C(n-1)\delta^2}{(\delta_1 + i\delta)^n} &= C(n-1)\delta^{2-n} \sum_{i=1}^{N-2} \frac{1}{\left(\frac{\delta_1}{\delta} + i\right)^n} \\ &\leq C(n-1)\delta^{2-n} \sum_{i=1}^{N-2} \int_{x=0}^{+\infty} \frac{1}{\left(\frac{\delta_1}{\delta} + x\right)^n} dx \\ &= C(n-1)\delta^{2-n} \cdot \frac{1}{n-1} \left(\frac{\delta}{\delta_1}\right)^{n-1} \\ &= \frac{C\delta}{\delta_1^{n-1}} \\ &\leq \epsilon. \end{aligned}$$

Combining the above, we have:

$$\frac{D_{\text{KL}}(q||p)}{L \log |\mathcal{V}|} \leq 4\epsilon + \frac{\epsilon_{\text{learning}}}{\log |\mathcal{V}|}.$$

Meanwhile, the time step is limited by:

$$N = 1 + \frac{1-\delta_1}{\delta} = O\left(\frac{n-1}{\epsilon^n}\right),$$

and the lower bound for L :

$$L \geq \frac{3}{\delta\epsilon^{\frac{1}{2}}} = \frac{3C(n-1)}{\epsilon^{n+\frac{1}{2}}}.$$

□

Combining the above lemmas, we can prove Theorem 4.2 by breaking the expression of $\log \text{TER}(p)$ into two parts.

Theorem B.13 (TER Bounds for n -Gram Language Generation). *For any n -gram language q and any $\epsilon > 0$, let p_θ denote the reverse model and L denote the sequence length. The distribution over sequences generated by p_θ is denoted as p . For any $L > O\left(\frac{n-1}{\epsilon^{n+0.5}}\right)$, under Assumption 4.1, there exists a masking schedule α_t such that, with $N = O\left(\frac{n-1}{\epsilon^n}\right)$ sampling steps, the perplexity of the MDM is upper-bounded by:*

$$\log \text{TER}(p) \leq \log \text{TER}(q) + \epsilon_{\text{learning}} + 4\epsilon \log |\mathcal{V}|.$$

Proof. By Lemma B.12, for any $L > O\left(\frac{n-1}{\epsilon^{n+0.5}}\right)$, there exists a masking schedule α_t with $N = O\left(\frac{n-1}{\epsilon^n}\right)$ sampling steps satisfying:

$$\frac{D_{\text{KL}}(q||p)}{L \log |\mathcal{V}|} \leq 4\epsilon + \frac{\epsilon_{\text{learning}}}{\log |\mathcal{V}|}.$$

In other words:

$$\frac{1}{L} \mathbb{E}_{\mathbf{x} \sim q} \log \frac{q(\mathbf{x})}{p(\mathbf{x})} \leq 4\epsilon \log |\mathcal{V}| + \epsilon_{\text{learning}}.$$

By the definition of TER, we have:

$$\log \text{TER}(p) = \mathbb{E}_{\mathbf{x} \sim q} - \frac{\log p(\mathbf{x})}{|\mathbf{x}|} = \frac{1}{L} \mathbb{E}_{\mathbf{x} \sim q} \left(-\log q(\mathbf{x}) + \log \frac{q(\mathbf{x})}{p(\mathbf{x})} \right).$$

Note that:

$$\log \text{TER}(q) = \mathbb{E}_{\mathbf{x} \sim q} - \frac{\log q(\mathbf{x})}{|\mathbf{x}|} = \frac{1}{L} \mathbb{E}_{\mathbf{x} \sim q} - \log q(\mathbf{x}).$$

We can obtain:

$$\log \text{TER}(p) \leq \log \text{TER}(q) + \epsilon_{\text{learning}} + 4\epsilon \log |\mathcal{V}|.$$

□

C. Proof for Theorem 4.3 and Theorem 4.4

C.1. Proof for Theorem 4.3

In this section, we aim to derive the upper bound for the SER of generated sequences with sufficient reverse steps. First, we argue that, given a making schedule α_t , with sufficient steps, the probability of sampling multiple locations in the sequence at the same time can be very low.

Lemma C.1 (Low Probability of Simultaneous Sampling with Sufficient Steps). *Given a sequence of length L and a masking schedule α_t . For any $\epsilon > 0$, there exists N_0 , such that for any $N \geq N_0$, with N reverse steps, the probability p_{mul} of sampling multiple locations in the sequence at the same time satisfies:*

$$p_{\text{mul}} < \epsilon.$$

Proof. By Lemma B.10, we know that the probability of a location being sampled at time step $t_i = \frac{N-i}{N}$ is:

$$\delta_i = \alpha_{t_i} - \alpha_{t_{i-1}} = \alpha_{\frac{N-i}{N}} - \alpha_{\frac{N-i+1}{N}}.$$

Since all the locations are sampled independently, for two distinct locations $i \neq j$ in the sequence, the probability that i and j are sampled simultaneously is:

$$p_{i,j} = \sum_{i=1}^N \delta_i^2.$$

Summing up $p_{i,j}$, the probability of having two locations a=sampled simultaneously can be bounded by:

$$p_{\text{mul}} \leq \frac{L(L-1)}{2} \cdot \sum_{i=1}^N \delta_i^2$$

Since α_t is continuous on $[0, 1]$, we know that it is uniformly continuous. Therefore, for any $\epsilon > 0$, there exists $N_0 > 0$ that satisfies:

$$|\alpha_x - \alpha_y| < \frac{2\epsilon}{L(L-1)}, \quad \forall x, y \in [0, 1], |x - y| < \frac{1}{N_0}.$$

In this case, for $N > N_0$, we know that:

$$|\delta_i| = |\alpha_{\frac{N-i}{N}} - \alpha_{\frac{N-i+1}{N}}| < \frac{2\epsilon}{L(L-1)}, \quad \forall i \in [N].$$

Combining with the fact that $\sum_{i=1}^N \delta_i = 1$, we can obtain:

$$p_{\text{mul}} \leq \frac{L(L-1)}{2} \cdot \sum_{i=1}^N \delta_i \cdot \max_{j \in [N]} \delta_j < \epsilon.$$

□

Next, we consider the SER increase due to the learning error. Specifically, we only investigate the case where all the locations are sampled at different steps.

Lemma C.2 (Accurate Step-by-Step Generation with Low Learning Error). *Let q denote any HMM, and let p_θ represent the reverse model under an arbitrary masking schedule, where L is the sequence length. Let p denote the distribution over sequences generated by p_θ . Under Assumption 4.1 with a learning error $\epsilon_{\text{learning}} < \frac{\delta}{L}$, $\delta > 0$, and given an instance of reverse process $\tau = (\mathcal{M}_1, \mathcal{M}_2, \dots, \mathcal{M}_N)$ with $|\mathcal{M}_i| \leq 1$, let p_{acc} denote the probability of generating a valid sequence. Then p_{acc} satisfies:*

$$p_{\text{acc}} \geq e^{-\delta}.$$

Proof. Since $|\mathcal{M}_i| \leq 1$, we only need to consider the steps where one token is sampled. Let $\tilde{\mathbf{x}}_t$ denote the previously sampled tokens, and \tilde{x}_t denote the token sampled at the current step. If $\tilde{\mathbf{x}}_t$ is can later form a valid sequence, let \mathcal{X}_t denote the set of valid choices for \tilde{x}_t . In other words, if $\tilde{x}_t \in \mathcal{X}_t$, then the combination of $\tilde{\mathbf{x}}_t$ and \tilde{x}_t is can later form a valid sequence, or more intuitively:

$$q_{0|t}(\tilde{x}_t | \tilde{\mathbf{x}}_t) > 0.$$

Under Assumption 4.1, we know that:

$$D_{\text{KL}}(q_{0|t}(x_t | \tilde{\mathbf{x}}_t) || p_\theta(x_t | \tilde{\mathbf{x}}_t)) < \epsilon_{\text{learning}}.$$

Since it is assumed that $0 \log 0 = 0$, we have:

$$\sum_{x_t \in \mathcal{X}_t} q_{0|t}(x_t | \tilde{\mathbf{x}}_t) \log \frac{q_{0|t}(x_t | \tilde{\mathbf{x}}_t)}{p_\theta(x_t | \tilde{\mathbf{x}}_t)} < \epsilon_{\text{learning}}.$$

Equivalently, we have:

$$-\epsilon_{\text{learning}} < \sum_{x_t \in \mathcal{X}_t} q_{0|t}(x_t | \tilde{\mathbf{x}}_t) \log \frac{p_\theta(x_t | \tilde{\mathbf{x}}_t)}{q_{0|t}(x_t | \tilde{\mathbf{x}}_t)}.$$

Due to the concavity of $\log x$, by Jensen's Inequality, we can obtain:

$$\sum_{x_t \in \mathcal{X}_t} q_{0|t}(x_t | \tilde{\mathbf{x}}_t) \log \frac{p_\theta(x_t | \tilde{\mathbf{x}}_t)}{q_{0|t}(x_t | \tilde{\mathbf{x}}_t)} \leq \log \left(\sum_{x_t \in \mathcal{X}_t} q_{0|t}(x_t | \tilde{\mathbf{x}}_t) \cdot \frac{p_\theta(x_t | \tilde{\mathbf{x}}_t)}{q_{0|t}(x_t | \tilde{\mathbf{x}}_t)} \right) = \log \sum_{x_t \in \mathcal{X}_t} p_\theta(x_t | \tilde{\mathbf{x}}_t).$$

Therefore, the probability that each step remains valid satisfies:

$$\sum_{x_t \in \mathcal{X}_t} p_\theta(x_t | \tilde{\mathbf{x}}_t) \geq e^{-\epsilon_{\text{learning}}} \geq e^{-\frac{\delta}{L}}.$$

Since there are L locations in the sequence, the probability of generating a valid sequence is bounded by:

$$p_{\text{acc}} \geq (e^{-\frac{\delta}{L}})^L = e^{-\delta}.$$

□

Combining the above lemmas, we can derive the upper bound of SER by taking sufficient reverse steps and small learning error.

Theorem C.3 (Accurate Generation of HMM with Sufficient Steps). *Let q denote any HMM, and let p_θ represent the reverse model under an arbitrary masking schedule, where L is the sequence length. Let p denote the distribution over sequences generated by p_θ . Under Assumption 4.1 with a learning error $\epsilon_{\text{learning}} < O(\frac{\delta}{L})$, and given a sufficient number of reverse steps, the sequence error rate $\text{SER}(p)$ of the generated text satisfies*

$$\text{SER}(p) \leq \delta.$$

Proof. For $\delta > 0$, we know that:

$$1 - \delta < c.$$

By Lemma C.1, given the masking schedule α_t , there exists N_0 , for $N > N_0$ and N reverse steps, the probability of sampling multiple locations in the sequence at the same time is bounded by:

$$p_{\text{mul}} < 1 - \frac{1 - \delta}{e^{-\delta}}.$$

In other words, the probability of sampling all the locations at different steps is at least $\frac{1-\delta}{e^{-\delta}}$. By Lemma C.2, for each reverse process which satisfies that all the locations are sampled at different steps, the probability of generating a valid sequence is lower bounded by:

$$p_{\text{acc}} \geq e^{-\delta}.$$

Therefore, the sequence error rate SER satisfies:

$$\text{SER}(p) \leq 1 - \frac{1 - \delta}{e^{-\delta}} \cdot e^{-\delta} = \delta.$$

□

C.2. Proof for Theorem 4.4

In the section, we aim to find an example (Example C.7) with high sequence error rate. To present this example, we begin with a special class of languages defined under the interval setting:

Definition C.4 (Interval Setting). Consider a sequence of length L , which is divided equally into M intervals $\mathcal{I}_1, \mathcal{I}_2, \dots, \mathcal{I}_M$, each of length $l = \frac{L}{M} \geq 2$. Given a masking schedule α_t , an instance of reverse process $\tau = (\mathcal{M}_1, \mathcal{M}_2, \dots, \mathcal{M}_N)$ is defined by Definition B.1. For any two locations within different intervals, their corresponding tokens are independent from each other. In other words, let $\tilde{\mathbf{x}}_i^{(j)}$ denote the new tokens in $\mathcal{M}_i \cap \mathcal{I}_j$, $\tilde{\mathbf{x}}_{<i}^{(j)}$ denote the previously sampled tokens in $\mathcal{M}_{<i} \cap \mathcal{I}_j$, and p denote the distribution over sequences generated by the reverse model with reverse process τ , then for time step $t_i = \frac{N-i}{N}$:

$$p(\tilde{\mathbf{x}}_i^{(j)} | \tilde{\mathbf{x}}_{<i}) = p(\tilde{\mathbf{x}}_i^{(j)} | \tilde{\mathbf{x}}_{<i}^{(j)}).$$

In this case, we have:

$$p(\mathbf{x}) = \prod_{j=1}^M p(\mathbf{x}^{(j)}) = \prod_{j=1}^M \prod_{i=1}^N p(\tilde{\mathbf{x}}_i^{(j)} | \tilde{\mathbf{x}}_{<i}^{(j)}).$$

We denote the above setting as $\text{Inter}(L, l, \alpha_t)$.

Under the interval setting defined above, we can control the probability of sampling simultaneously in the same interval.

Lemma C.5 (Simultaneous Sampling Probability for an Interval). *Consider the interval setting $\text{Inter}(L, l, \alpha_t)$. For each interval \mathcal{I}_j of length l , let h_j denote the probability that all the locations in \mathcal{I}_j are sampled in different time steps. Then, h_j can be bounded by:*

$$h_j \leq 1 - \frac{1}{N}.$$

Proof. Let $\delta_i = \alpha_{t_i} - \alpha_{t_{i-1}}$. Similar to Lemma B.10, we know that δ_i is the probability of a location being sampled at time step t_i . Take the first location in $|\mathcal{I}_j|$, denote it as X_1 , and let X_2, \dots, X_l denote the rest $l - 1$ locations in \mathcal{I}_j . If X_1 is sampled at step t_i , then X_2, \dots, X_l must be sampled at time steps other than t_i . Therefore, h_j can be bounded by:

$$h_j \leq \sum_{i=1}^N \delta_i (1 - \delta_i)^{l-1} \leq \sum_{i=1}^N \delta_i (1 - \delta_i).$$

Let $f(\delta) = \delta(1 - \delta)$. Note that we have:

$$f''(\delta) = -2 \leq 0,$$

which indicates that $f(\delta)$ is concave. Using Jensen's Inequality, we can obtain:

$$h_j \leq \sum_{i=1}^N f(\delta_i) \leq N f\left(\frac{1}{N}\right) = 1 - \frac{1}{N}.$$

□

Using the above lemma, if we assume that sampling simultaneously in one interval increases SER, then we can derive an lower bound for $\text{SER}(p)$.

Lemma C.6 (SER bound for Interval Setting). *Consider the interval setting $\text{Inter}(L, l, \alpha_t)$. Assume that sampling simultaneously in the same interval introduces an error with probability at least p_0 , and other actions do not reduce error. In other words, if two locations in an interval are both sampled at step t_i , then there is a probability of p_e that the sequence will not be accurate afterwards. In this case, let p denote the distribution over sequences of length L generated by the reverse model with masking schedule α_t and N reverse steps. We have the following bound for SER:*

$$\text{SER}(p) \geq 1 - \left(1 - \frac{p_e}{N}\right)^{L/l}.$$

Proof. By Lemma C.5, we can obtain that for each interval \mathcal{I}_j , the probability $p_{\text{error}}^{(j)}$ of generating an error in \mathcal{I}_j is lower-bounded by:

$$p_{\text{error}}^{(j)} \geq p_e (1 - h_j) \geq \frac{p_e}{N}.$$

Due to the independence between different intervals, the accuracy $\text{SER}(p)$ can be calculated as:

$$\text{SER}(p) = 1 - \prod_{j=1}^M (1 - p_{\text{error}}^{(j)}).$$

Therefore, we have the bound:

$$\text{SER}(p) \geq 1 - \left(1 - \frac{p_e}{N}\right)^{L/l}.$$

□

To show that the above setting is reasonable and achievable, we give the following example, which is later shown to be the example we are looking for.

Example C.7. Consider a sequence of length L , which is divided equally into M intervals, each of length $l = L/M$. Denote the k -th interval as $\mathcal{I}_k = [1 + (k - 1)l, kl]$. The tokens x_i , $1 \leq i \leq L$ in the sequence satisfy the following rules:

- Each x_i takes values in the set $\mathcal{A} = \{a_1, \dots, a_{2^{l-1}}\}$. For each $a_j \in \mathcal{A}$, there corresponds a vector $v_j = (v_{j,1}, \dots, v_{j,l-1}) \in \{0, 1\}^{l-1}$, where $(v_{j,1} \dots v_{j,l-1})_2$ is the binary expression for $j - 1$. Thus, each random variable x_i corresponds to a random vector $(v_1^{(i)}, \dots, v_{l-1}^{(i)})$, where $v_j^{(i)} \in \{0, 1\}$ for $j = 1, \dots, l - 1$.
- For $i \in \mathcal{I}_k$ and $j \in \mathcal{I}_s$, if $k \neq s$, then x_i and x_j are independent.

- For $i, j \in \mathcal{I}_k$ such that $i < j$, let $i' = i - (s - 1)l$ and $j' = j - (s - 1)l$. Then, x_i and x_j are the i' -th and j' -th elements in interval \mathcal{I}_k , respectively. The corresponding binary components satisfy $v_{j'-1}^{(i)} = v_{i'}^{(j)} \sim \text{Bernoulli}(\frac{1}{2})$, which is independent of all other $v_t^{(s)}$.

In this setup, each interval \mathcal{I}_k contains $\frac{l(l-1)}{2}$ pairs of mutually independent random variables. Given an arbitrary masking schedule α_t , this setting is consistent with Definition C.4. Let q denote the data distribution described above.

Under Assumption 4.1, we only need to examine the case where \mathbf{x}_t has no error. By Lemma A.3, we know that:

$$\|q_{0|t}(x_0^i | \mathbf{x}_t) - p_\theta(x_0^i | \mathbf{x}_t)\|_1 \leq \sqrt{2D_{\text{KL}}(q_{0|t}(x_0^i | \mathbf{x}_t) \| p_\theta(x_0^i | \mathbf{x}_t))} \leq \sqrt{2\epsilon_{\text{learning}}}.$$

Let \mathcal{M} denote the set of previously sampled locations. For q and any unsampled location in interval \mathcal{I} , all of the potential tokens x at this location which is consistent with \mathbf{x}_t have the same probability:

$$q(x|\mathbf{x}_t) = \frac{1}{2^{l-1-|\mathcal{M} \cap \mathcal{I}|}}.$$

If two locations x_i, x_j within the same interval \mathcal{I} are sampled simultaneously, ignoring the possible inconsistency with previously sampled tokens (since error can not be reduced), the independence of the random variable pairs implies that the probability of generating an error is lower-bounded by:

$$p_e \geq \left(\frac{1}{2} + e_1\right)\left(\frac{1}{2} + e_2\right) + \left(\frac{1}{2} + e_3\right)\left(\frac{1}{2} + e_4\right)$$

where $\frac{1}{2}$ implies the probability (for q) of letting $v_{i'}^{(j)}$ or $v_{j'-1}^{(i)}$ to be 0 or 1, and e_1, e_2, e_3, e_4 satisfies:

$$\begin{aligned} |e_1| + |e_3| &= \|q_{0|t}(x_0^i | \mathbf{x}_t) - p_\theta(x_0^i | \mathbf{x}_t)\|_1 \\ |e_2| + |e_4| &= \|q_{0|t}(x_0^j | \mathbf{x}_t) - p_\theta(x_0^j | \mathbf{x}_t)\|_1 \end{aligned}$$

Thus, we know that:

$$p_e \geq \frac{1}{2} - (|e_1| + |e_2| + |e_3| + |e_4|) \geq \frac{1}{2} - 2\sqrt{2\epsilon_{\text{learning}}}.$$

In other words, this is consistent with the setting Lemma C.6, with an error probability $p_e = \frac{1}{2} - 2\sqrt{2\epsilon_{\text{learning}}}$.

Although the example above seems a bit tricky, it can actually be modified into the form of an HMM, a commonly considered structure for generative models.

Note C.8 (HMM Form of Example C.7). The setting described in Example C.7 can be alternatively modeled as a Hidden Markov Model (HMM), where the observation space is $\mathcal{O} = \mathcal{A}$, and the state space is $\mathcal{S} = \{(i, A^{(i)}) | A^{(i)} \in \mathbb{R}^{(l-1) \times (l-1)}, i = 1, \dots, l\}$. Here, i represents the current position within the interval, and $A^{(i)}$ is an upper triangular matrix with entries taking values of 0 or 1. For $j \leq i$, the j -th row of $A^{(i)}$ encodes the values sampled by the variable pairs formed between the j -th position and all its subsequent positions in the interval. For $j > i$, the j -th row of $A^{(i)}$ is set to 0.

Given the current state $s = (i, A^{(i)})$, the state transition and emission process can be describe as follows:

- The observation o_i corresponds to the $i - 1$ -th column and the i -th row of the matrix $A^{(i)}$, where the values of variable pairs relevant to the i -th position within the interval are encoded. Specifically, we know that $o_i \in \mathcal{A}$ corresponds to a vector $v_i = (v_{i,1}, \dots, v_{i,l-1})$, where

$$v_{i,j} = \begin{cases} A_{j,i-1}^{(i)}, & j < i, \\ A_{i,j}^{(i)}, & j \geq i. \end{cases}$$

- If $i < l$, the next state is $s' = (i, A^{(i+1)})$, where the first i rows of $A^{(i+1)}$ is the same as $A^{(i)}$, and $A_{i+1,j}^{(i+1)} \sim \text{Bernoulli}(\frac{1}{2})$ i.i.d. for $j = i + 1, \dots, l - 1$, with the remaining entries set to 0.

- If $i = l$, the next state resets to $s' = (1, A^{(1)})$, where the entries in the first row are independently sampled from Bernoulli($\frac{1}{2}$), and other entries are set to 0.

The size of the observation space is given by $|\mathcal{O}| = |\mathcal{A}| = 2^{l-1}$. The size of the state space is computed as:

$$|\mathcal{S}| = \sum_{i=1}^l 2^{(2l-i-1)i/2} \leq l \cdot 2^{l(l-1)/2}.$$

The above Note gives the HMM form of Example C.7. In fact, with appropriate adjustments, it can be further modified into an n-gram language. Using the HMM defined above, we can prove Theorem 4.4.

Theorem C.9 (SER Bound for HMM Generation). *There exists an HMM q over a vocabulary of size 16 that satisfies the following conditions: for any reverse model p_θ under Assumption 4.1 with $\epsilon_{\text{learning}} < \frac{1}{128}$, and any masking schedule α_t , let p denote the distribution over sequences generated by p_θ . There exists a constant C such that if the number of sampling steps satisfies $N = CL$, where L is the sequence length, the SER of the generated text is lower-bounded by:*

$$\text{SER}(p) > \frac{1}{2}.$$

Proof. Take the HMM described in Note C.8, and set $l = 5$, $N = CL$. The vocabulary is the observation space \mathcal{O} which satisfies $|\mathcal{O}| = 2^{l-1}$. By Lemma C.6, for any masking schedule α_t , we have:

$$\text{SER}(p) \geq 1 - \left(1 - \frac{p_e}{N}\right)^{L/l}.$$

As illustrated in Example C.7:

$$p_e = \frac{1}{2} - 2\sqrt{2\epsilon_{\text{learning}}}.$$

Therefore, take $N = CL$, and let $y = \frac{CL}{p_e}$, we have:

$$\text{SER}(p) \geq 1 - \left[\left(1 - \frac{1}{y}\right)^y \right]^{\frac{p_e}{Cl}}.$$

Since $(1 - \frac{1}{y})^y$ is decreasing, and apparently $y \geq \frac{Cl}{p_e}$, we know that:

$$\text{SER}(p) \geq \frac{p_e}{Cl}.$$

Let $C = \frac{2p_e}{l+1}$, we can get the upper bound:

$$\text{SER}(p) > \frac{1}{2}.$$

In this way:

$$C = \frac{2p_e}{l+1} = \frac{\frac{1}{2} - 2\sqrt{2\epsilon_{\text{learning}}}}{6} \geq \frac{1}{24} = O(1).$$

□

D. Extend to Efficient Sampling Strategies

In Sahoo et al. (2024) and Ou et al. (2024), an efficient sampling strategy `ddpm_cache` is proposed, which can reduce the sampling time by a constant order of magnitude. Specifically, this sampler is approximately 3-4 times faster than previously used samplers when the number of sampling steps is large. In this section, we discuss the influence of `ddpm_cache` on our conclusions under different sampling steps.

First, we briefly introduce the principles of `ddpm_cache`. It utilizes the observation that if no locations are sampled at a given step, the sequence remains unchanged. Consequently, when the reverse model is not conditioned on time, the cached value computed during the first time this sequence went through the reverse model can be reused, instead of going through the reverse model again.

This sampling strategy does not affect our main theorems, as they are based solely on the sampled locations at each step, while unsampled locations are not considered. As for the evaluation metrics for computational efficiency in our experiments, we break it down into the following two cases:

1. When the number of sampling steps is much smaller than the sequence length, which is the primary scenario we focus on, the expectation of steps where no new locations are sampled is relatively low, resulting in a computational cost that is nearly linear with respect to the number of sampling steps.
2. As the number of sampling steps becomes larger, the computational cost is mainly dependent on the number of valid steps where at least one location is sampled. As a matter of fact, the expectation of the number of valid steps increases as the number of sampling steps increases, and the maximum number of valid steps is equal to the number of sampling steps. In this case, the MDMs offer no computational advantage over auto-regressive models.

Based on the above conclusions, we can find that for tasks requiring a low TER, using `ddpm_cache` can further accelerate the generation of MDMs, suggesting high efficiency. Conversely, for tasks that demand a low SER, we have shown that the number of sampling steps need to be large enough, such that MDMs can not generate with low cost even when using `ddpm_cache`. Therefore, we extend our findings to MDMs with efficient sampling strategies.

E. Experiment Details

In this section, we will present the details of the experiments.

E.1. Data Generation

We evaluate the MDMs in a variety of formal languages, including n -gram languages and HMMs. For each formal language, parameters are generated through random sampling, we present the sampling algorithm in Algorithm 1 and Algorithm 2. It is notable that to add some deterministic to the language model in the evaluation of SER, we add the parameter of `thres` to prune the tail probabilities, making sure the language model only generates the correct sequence. For the evaluation of TER, we set the `thres` to be 0, for the well definition of generative perplexity. The detailed parameters to generate the formal languages are listed in Table 1.

Algorithm 1 Generate n -gram Language Model

Input:

`n`: number of grams
`vocab_size`: size of vocabulary
`temp`: temperature (controls randomness, higher indicates more randomness)
`thres`: threshold for pruning small probabilities

Output: n -gram language model with parameters:

T : transition probability matrix ($\text{vocab_size}^{n-1} \times \text{vocab_size}$)

`Init_dist`: initial state distribution

- 1: `Init_dist` \leftarrow `rand(hidden_states_num)`
 - 2: `Init_dist` \leftarrow `Init_dist` / $\sum(\text{Init_dist})$
 - 3: $T \leftarrow \text{randn}(\text{vocab_size}^{n-1}, \text{vocab_size}) \times \text{randomness}$
 - 4: $T \leftarrow \text{softmax}(T)$
 - 5: **if** `thres` > 0 **then**
 - 6: $T[\text{where}(T < \text{thres})] \leftarrow 0$
 - 7: $T \leftarrow T / \text{rowsum}(T)$
 - 8: **end if**
 - 9: **return** T and `Init_dist`
-

Table 1. Generation Parameters for Different Language Models

Parameter	2-gram	3-gram	4-gram	HMM
vocabulary size	8	8	8	8
Hidden States (n)	N/A	N/A	N/A	32
Temperature	2	2	2	3.2
Threshold	0.008	0.008	0.005	0.003

Algorithm 2 Generate Hidden Markov Model

Input:

n : number of hidden states
 vocab_size: size of vocabulary
 randomness: temperature parameter to control probability distributions
 thres: threshold for pruning small transition probabilities

Output: HMM with parameters:

A : state transition matrix ($n \times n$)
 B : emission probability matrix ($n \times (\text{vocab_size} + 1)$)
 Init_dist: initial state distribution (n -dimensional)

- 1: hidden_states_num $\leftarrow n$
- 2: Init_dist $\leftarrow \text{rand}(\text{hidden_states_num})$
- 3: Init_dist $\leftarrow \text{Init_dist} / \sum(\text{Init_dist})$
- 4: $A \leftarrow \text{randn}(\text{hidden_states_num}, \text{hidden_states_num}) \times \text{randomness}$
- 5: $A \leftarrow \text{softmax}(A)$
- 6: **if** thres > 0 **then**
- 7: $A[\text{where}(A < \text{thres})] \leftarrow 0$
- 8: $A \leftarrow A / \text{rowsum}(A)$
- 9: **end if**
- 10: $B \leftarrow \text{randn}(\text{hidden_states_num}, \text{vocab_size}) \times \text{randomness} \times 2.5$
- 11: $B \leftarrow \text{softmax}(B)$
- 12: $B[\text{where}(B < 0.05)] \leftarrow 0$
- 13: $B \leftarrow B / \text{rowsum}(B)$
- 14: $B \leftarrow \text{concat}(B, \text{ones}(\text{hidden_states_num}, 1) / \text{hidden_states_num})$
- 15: **return** A, B , and Init_dist

E.2. Model Training and Testing

In our experiments of formal languages, all training was conducted on NVIDIA A100 GPUs. The model architectures and train configurations are listed in Table 2 and Table 3. The training configuration of the auto-regressive model is listed in Table 4.

Model Configuration	
Hidden Size	512
Sequence Length	512
Number of Layers	8*
Attention Heads	8

*For the 4-gram model, the number of layers is 10.

Table 2. Model Configuration for the Formal Language Tasks

Training Configuration for MDMs	
Epochs	20
Learning Rate	3e-4
Optimizer	AdamW
β_1	0.9
β_2	0.999
Learning Rate Scheduler	Cosine Scheduler with Warmup
Warmup Ratio	0.1

Table 3. Training Configuration for MDMs on the Formal Language Tasks

Training Configuration for Auto-regressive Models	
Epochs	20
Learning Rate	3e-4
Optimizer	AdamW
β_1	0.9
β_2	0.999
Learning Rate Scheduler	Cosine Scheduler with Warmup
Warmup Ratio	0.1

Table 4. Training Configuration for Auto-regressive Models on the Formal Language Tasks

Speedup Testing Settings	
GPU	Nvidia RTX 4090
Batch Size	16
Sequence Length	512
Testing Model Configuration	In Table 2

Table 5. Setting for the experiments to test the speedup of MDMs under different sampling steps compare to auto-regressive models.